Functional characterization of the *GhNRT2.1e* gene reveals its significant role in improving nitrogen use efficiency in *Gossypium hirsutum*

Xinmiao Zhang[1], Jiajia Feng[1], Ruolin Zhao[1], Hailiang Cheng[1], Javaria Ashraf[2], Qiaolian Wang[1], Limin Lv[1], Youping Zhang[1], Guoli Song[1*], Dongyun Zuo[1*]

[1] State Key Laboratory of Cotton Biology, Institute of Cotton Research, Chinese Academy of Agricultural Sciences, Anyang, Henan, China

[2] Department of Plant Breeding and Genetics, Faculty of Agriculture and Environment, The Islamia University of Bahawalpur, Punjab, Pakistan

* Co-Corresponding Author:
Guoli Song
Anyang, Henan, 455000, China
Email address: sglzms@163.com
Dongyun Zuo
Anyang, Henan, 455000, China
Email address: zdy041@163.com

Abstract

Background. Nitrate is the primary type of nitrogen available to plants, which is absorbed and transported by nitrate transporter 2 (NRT2) at low nitrate conditions.

Methods. Genome-wide identification of *NRT2* genes in *G. hirsutum* was performed. Gene expression patterns were revealed using RNA-seq and qRT-PCR. Gene functions were characterized using overexpression in *A. thaliana* and silencing in *G. hirsutum*. Protein interactions were verified by yeast two-hybrid and luciferase complementation imaging (LCI) assays.

Results. We identified 14, 14, 7, and 7 *NRT2* proteins in *G. hirsutum*, *G. barbadense*, *G. raimondii*, and *G. arboreum*. Most NRT2 proteins were predicted in the plasma membrane. The *NRT2* genes were classified into four distinct groups through evolutionary relationships, with members of the same group similar in conserved motifs and gene structure. The promoter regions of *NRT2* genes included many elements related to growth regulation, phytohormones, and abiotic stresses. Tissue expression pattern results revealed that most *GhNRT2* genes were specifically expressed in roots. Under low nitrate conditions, *GhNRT2* genes exhibited different expression levels, with *GhNRT2.1e* being the most up-regulated. *Arabidopsis* plants overexpressing *GhNRT2.1e* exhibited increased biomass, nitrogen and nitrate accumulation, nitrogen uptake and utilization efficiency, nitrogen-metabolizing enzyme activity, and amino acid content under low nitrate conditions. In addition, *GhNRT2.1e*-silenced plants exhibited

38 suppressed nitrate uptake and accumulation, hampered plant growth, affected nitrogen
39 metabolism processes, and reduced tolerance to low nitrate. The results showed that *GhNRT2.1e*
40 could promote nitrate uptake and transport under low nitrate conditions, thus effectively
41 increasing nitrogen use efficiency (NUE). We found that GhNRT2.1e interacts with GhNAR2.1
42 by yeast two-hybrid and LCI assays.

43 **Discussion.** Our research lays the foundation to increase NUE and cultivate new cotton varieties
44 with efficient nitrogen use.

45 **Keywords.** *NRT2*; NUE; Gene family; Expression pattern; High-affinity nitrate transporter;
46 *Gossypium hirsutum*

47 Introduction

48 As an essential nutrient element, nitrogen (N) participates in the composition of nucleic acids,
49 amino acids, chlorophyll, and many secondary metabolites (Akbudak et al., 2022). In agricultural
50 production, nitrogen fertilizers are often over-applied to increase yields. However, less nitrogen
51 fertilizer is absorbed by plants, and the rest is retained in soil or leaches into groundwater,
52 causing increase in production costs, waste resources, and environmental problems (Zhou et al.,
53 2022). Therefore, preventing the over-application of nitrogen fertilizer and increasing nitrogen
54 use efficiency (NUE) is significant in protecting the environment and enhancing yield.

55   There are three forms of nitrogen available to plants including nitrate (NO_3^-), ammonium
56 (NH_4^+), and organic nitrogen, among which NO_3^- is the most important form absorbed and
57 utilized by plants (Ren et al., 2020). Nitrate absorption and transportation are primarily based on
58 nitrate transporters (*NRTs*) (You et al., 2022). To accommodate the different nitrate
59 concentrations in soil, plants have evolved low-affinity transport system (LATS) and high-
60 affinity transport system (HATS)(Li et al., 2007; Léran et al., 2014). LATS mainly consists of
61 nitrate transporter 1/peptide transporter (*NRT1/PTR*), while nitrate transporter 2 (*NRT2*) is part of
62 HATS (Dechorgnat et al., 2011).

63   *NRT2* genes are essential for improving NUE through efficient uptake and transport of
64 nitrate. *NRT2* genes have been investigated in *A. thaliana* (Orsel et al., 2002), rice (Cai et al.,
65 2008), barley (Trueman et al., 1996), soybean (Amarasinghe et al., 1998), and maize (Lupini et
66 al., 2016). In *Arabidopsis*, seven *NRT2* members (*AtNRT2.1-AtNRT2.7*) were identified.
67 *AtNRT2.1* is primarily expressed in roots and significantly affects nitrate uptake (Wirth et al.,
68 2007). Interestingly, elevated expression of *AtNRT2.2* compensated for partial loss of nitrate
69 uptake when *AtNRT2.1* lost its ability to absorb nitrate (Li et al., 2007). *AtNRT2.4* is primarily
70 concerned with nitrate absorption in roots and transportation in the phloem (Kiba et al., 2012).
71 *AtNRT2.5* is expressed in leaves and roots, and its expression levels increase with the increase in
72 nitrogen starvation (Lezhneva et al., 2014). *AtNRT2.7* regulates nitrate storage in seeds (Chopin
73 et al., 2007). Most NRT2 proteins depend on nitrate assimilation related (NAR2) proteins, and in
74 *Arabidopsis*, most AtNRT2 proteins require binding to AtNAR2.1, whereas AtNRT2.7 can be
75 transported alone (Kotur et al., 2012). A similar situation was demonstrated in rice, where
76 OsNRT2.1, OsNRT2.2, and OsNRT2.3a are required to interact with OsNAR2.1, whereas
77 OsNRT2.3b and OsNRT2.4 can absorb and transport nitrate alone (Wei et al., 2018).

78   As a cash crop, the growth and yield of cotton are regulated by nitrogen. Therefore, we can
79   effectively improve cotton's nitrogen uptake and utilization efficiency by mining nitrogen-
80   efficient genes through molecular techniques (Magwanga et al., 2019). These essential genes will
81   help us to maintain cotton yield while reducing nitrogen fertilizer input. In this research, we
82   identified *GhNRT2* genes and determined their evolutionary relationships, physicochemical
83   properties, chromosomal location, gene duplication, collinearity relationship, conserved motifs,
84   gene structure and cis-acting elements. After low nitrogen treatment, we observed the expression
85   pattern of *GhNRT2* genes and found that *GhNRT2.1e* was the most up-regulated gene. We
86   characterized the *GhNRT2.1e* functions by overexpression in *A. thaliana* and silencing in *G.
87   hirsutum*. Furthermore, we validated the interaction between GhNRT2.1e and GhNAR2.1 by
88   yeast two-hybrid and LCI assays. This study lays a foundation for increasing NUE and breeding
89   new cotton cultivars with high nitrogen using efficiency.

Materials & Methods

90

91   **Plant Materials and Treatments.**
92   Cotton material used in the experiment was *G. hirsutum* L. TM-1. The seeds were germinated on
93   moist filter paper until two cotyledons appeared. The seedlings continued to grow in the
94   hydroponic conditions. Growing conditions were 16 hours light at 28°C and 8 hours dark at 25°C
95   with 60% relative humidity. We changed the Hoagland nutrient solution every five days. We
96   switched to the nitrogen-free nutrient solution at the three-leaf stage and continued for one week.
97   The NO_3^- concentration in Hoagland's nutrient solution was then adjusted to 0.25 mM for low
98   nitrogen treatment. Root tissues were collected at 0, 1, 3, 6, 12, 24, and 48 hours after treatment
99   and used for RNA extraction. The *Arabidopsis* ecotypes Columbia-0 and *Nicotiana benthamiana*
100   were grown in nutrient soil and vermiculite under light conditions for 16 hours at 22°C and 8
101   hours of dark conditions at 18°C with 60% relative humidity.

102   **Identification of *NRT2* genes in cotton**
103   To research *NRT2* family members in cotton, CottonGEN (http://www.cottongen.org/) was used
104   to download genome files of *G. barbadense* (ZJU_v1.1), *G. hirsutum* (ZJU_v2.1), *G. raimondii*
105   (JGI_v1.0), and *G. arboreum*(CRI_v1.0) (Yu et al., 2014). The protein sequences of AtNRT2 in
106   *Arabidopsis* were downloaded from TAIR (https://www.arabidopsis.org/) (Berardini et al., 2015).
107   We used AtNRT2 proteins as query sequences to identify NRT2 proteins in four cotton species
108   by BlastP (Chen et al., 2020). All identified NRT2 proteins were subjected to domain analysis by
109   Pfam (http://pfam.xfam.org/) (El-Gebali et al., 2019). We referred to the nomenclature of the
110   rapeseed *NRT2* genes for naming the cotton *NRT2* genes (Tong et al., 2020). The
111   physicochemical properties of NRT2 proteins including amino acid length, molecular weight
112   (MW) and isoelectric point (pI) were analyzed by ExPASy-ProtParam
113   (http://web.expasy.org/protparam/) (Wilkins et al., 1999). The subcellular localization of NRT2
114   proteins was predicted using WOLF-PSORT (https://wolfpsort.hgc.jp/) (Horton et al., 2007). The
115   transmembrane helices of GhNRT2 proteins were predicted by TMHMM 2.0 online server
116   (https://services.healthtech.dtu.dk/service.php?TMHMM-2.0/) (Krogh et al., 2001).

117   **Phylogenetic analysis, chromosomal location and synteny analysis of *NRT2* genes**

118 The evolutionary relationships of NRT2 proteins were indicated by phylogenetic analysis.
119 Multiple sequence alignment of NRT2 proteins in *A. thaliana*, *G. hirsutum*, *G. raimondii*, *G.*
120 *arboreum*, and *G. barbadense* was performed through ClustalW (Larkin et al., 2007). The
121 phylogenetic tree was constructed using the Neighbor-Joining (NJ) method in MEGA 7.0
122 software and drawn by iTOL (https://itol.embl.de/) (Kumar et al., 2016; Letunic & Bork, 2021).
123 Chromosome location of *NRT2* genes was acquired from the gff3 file downloaded by CottonGen
124 (https://www.cottongen.org/), and TBtools was used to visualize the distribution of *NRT2* genes
125 on chromosomes (Chen et al., 2020). The synteny relationship of *NRT2* genes was investigated
126 using MCScanX (Wang et al., 2012). To investigate the selection pressure between homologous
127 gene pairs, we used TBtools to calculate nonsynonymous substitution (Ka) and synonymous
128 substitution (Ks) rates for duplicated gene pairs (Chen et al., 2020).

129 **Gene structure, conserved motif and cis-acting elements analysis**

130 The structure of *GhNRT2* genes were investigated by GSDS (http://gsds.gao-lab.org/) (Hu et al.,
131 2015). The conserved motifs of GhNRT2 proteins were predicted by MEME (http://meme-
132 suite.org/tools/meme) (Bailey et al., 2015). The 2000 bp upstream sequences of the initiation
133 codons of *GhNRT2* genes were extracted, and predicted cis-acting elements using the
134 PlantCARE database (http://bioinformatics.psb.ugent.be/webtools/plantcare/html/) (Lescot et al.,
135 2002).

136 **Analysis of expression patterns of *GhNRT2* genes**

137 To analyze the expression patterns of *GhNRT2* genes in different tissues, we downloaded RNA-
138 seq data (accession number: PRJNA490626) of roots, stems, leaves, petals, receptacles, sepals,
139 bracts, ovules, and fibers of *G. hirsutum* TM-1 from the Cotton Omics Database
140 (http://cotton.zju.edu.cn) (Hu et al., 2019). The expression levels of *GhNRT2* genes were
141 visualized by TBtools based on log2 (FPKM+1) values (Chen et al., 2020). To validate the
142 results of RNA-seq, we collected roots, stems, and leaves tissues from TM-1 plants at the three-
143 leaf stage for RNA extraction.

144 **RNA extraction and qRT-PCR analysis**

145 We obtained total RNA by RNAprep Pure Plant kit (Tiangen, Beijing, China) and measured the
146 quantity and quality of RNA samples by spectrophotometer. The RNA was reverse transcribed
147 into cDNA using StarScript II First-strand cDNA Synthesis kit (GenStar, Beijing, China). The
148 quality of the cDNA was examined by PCR using the *GhActin* gene as an internal gene, and
149 better quality cDNA was used for qRT-PCR. The qRT-PCR was performed using fluorescence
150 quantitative kit 2×RealStar Green Fast Mixture with ROX II (GenStar, Beijing, China), and the
151 *GhActin* gene was used as an internal gene. The experiment was performed with three replicates.
152 We calculated the relative expression levels of genes according to the $2^{-\Delta\Delta CT}$ method (Schmittgen
153 & Livak, 2008). For the accuracy of the results, we also selected the *GhHis3* gene as the internal
154 gene for verification. The results using *GhHis3* as an internal control were similar to those of
155 *GhActin*, indicating the accuracy of the results and the availability of both internal reference
156 genes for qRT-PCR analysis. Specific primers for all genes were designed by NCBI Primer-blast
157 (http://www.ncbi.nlm.nih.gov/tools/primer-blast/) (Table S1).

158 **Overexpression vector construction and transformation**

159   To characterize the function of *GhNRT2.1e*, we amplified the *GhNRT2.1e* gene using primers
160   PRI101-GhNRT2.1e-F (SalI) and PRI101-GhNRT2.1e-R (BamHI) (Table S1). The PCR
161   products were inserted into the pRI101 vector containing the Cauliflower mosaic virus 35S
162   promoter forming an overexpression recombinant. The *35S: GhNRT2.1e* overexpression
163   recombinant was transformed to wild-type *A. thaliana* (Colombia-0) through *Agrobacterium*
164   *tumefaciens* flower soaking method. 50 mg/L kanamycin was added to the MS medium for
165   screening transformed T1 and T2 generations (Clough & Bent, 1998). We extracted RNA and
166   genomic DNA from transgenic *A. thaliana* and used *AtActin* as an internal gene to test the
167   quality of cDNA and genomic DNA. We performed PCR analysis of genomic DNA from
168   transgenic *A. thaliana* using primers 35S: PRI101-F and PRI101-GhNRT2.1e-R (BamHI). After
169   PCR and qRT-PCR analysis in the T2 generation, the highly expressed T3 generation was used
170   for phenotypic research. *A. thaliana* grown in vermiculite were provided with 0.25 mM and 2.5
171   mM of nitrate, creating a nitrogen deficiency and normal supply. Plants were grown for six
172   weeks by irrigating with a nutrient solution once a week.

173   **Virus-induced gene silencing**

174   We performed virus-induced gene silencing (VIGS) using tobacco rattle virus (TRV) to further
175   investigate the function of *GhNRT2.1e* (Gao et al., 2011). A sequence fragment of the
176   *GhNRT2.1e* gene was amplified using specific primers VIGS-GhNRT2.1e-F (EcoRI) and VIGS-
177   GhNRT2.1e-R (BamHI) and inserted into the TRV2 vector to form TRV2:GhNRT2.1e (Table
178   S1). Negative controls were wild-type and TRV2:00, while the effectiveness of the vector was
179   tested by phytoene desaturase (PDS). Cotton seedlings were used for injection when both
180   cotyledons were fully expanded. The NO_3^- concentration was adjusted to 0.25 mM and 2.5 mM
181   to provide plants with nitrogen deficiency and normal supply. Two weeks after plant growth,
182   RNA from TRV2:GhNRT2.1e, TRV2:00, and WT was extracted, and the silencing efficiency of
183   *GhNRT2.1e* was determined by qRT-PCR.

184   **Plant physiological and biochemical evaluation**

185   We performed physiological and biochemical evaluations of *Arabidopsis* and VIGS plants. Plant
186   samples were dried, and the dry weight was measured using a balance. The relative chlorophyll
187   contents were measured with the SPAD analyzer. The Kjeldahl method measured the total
188   nitrogen contents (Singh et al., 2020). The salicylic acid method measured the nitrate content
189   (Zhao & Wang, 2017). Iqbal's method calculated total nitrogen accumulation, nitrogen utilization
190   efficiency (NUtE), and nitrogen uptake efficiency (NUpE) (Iqbal et al., 2020a). Nitrate reductase
191   (NR), glutamine synthetase (GS), and glutamate synthase (GOGAT) activities, as well as amino
192   acid content were measured by assay kits (Solarbio, Beijing, China). In addition, we measured
193   the activity of antioxidants and oxidants: superoxide dismutase (SOD), peroxidase (POD),
194   catalase (CAT), and malondialdehyde (MDA) by detection kits (Solarbio, Beijing, China).

195   **Yeast two-hybrid assay**

196   In *Arabidopsis*, the interaction between AtNRT2.1 and AtNAR2.1 has been verified. We used
197   the protein sequence of AtNAR2.1 to verify whether this interaction exists in *G. hirsutum*.
198   Finally, we selected the homolog of AtNAR2.1 and named it as GhNAR2.1. The interaction
199   between GhNRT2.1e and GhNAR2.1 was verified by yeast two-hybrid assays. The specific

200   primers pPR3-N-GhNRT2.1e-F (BamHI)/pPR3-N-GhNRT2.1e-R (EcoRI) and pBT3-C-
201   GhNAR2.1-F (XbaI)/pBT3-C-GhNAR2.1-R (NcoI) were used to amplify the *GhNRT2.1e* and
202   *GhNAR2.1* coding sequences and inserted them into the pPR3-N and pBT3-C vectors to form the
203   pPR3-N-GhNRT2.1e and pBT3-C-GhNAR2.1 constructs (Table S1). The two constructs were
204   transferred into yeast NMY51, the transformants formed were grown on an SD-LW medium, and
205   positive transformants were selected for serial dilution (10^0, 10^{-1}, 10^{-2}, 10^{-3}) (Liu et al., 2014).
206   The different yeast dilutions were cultured on SD-LW and SD-AHLW media at 30 °C.
207   **Luciferase complementation imaging assay**
208   To verify whether GhNRT2.1e and GhNAR2.1 interact in vivo, we tested by LCI assay. The
209   coding sequences of *GhNRT2.1e* and *GhNAR2.1* were amplified using the specific primers
210   nLUC-GhNRT2.1e-F (BamHI)/nLUC-GhNRT2.1e-R (SalI) and cLUC-GhNAR2.1-F
211   (BamHI)/cLUC-GhNAR2.1-R (SalI), and they were inserted into the nLUC and cLUC vectors to
212   form the nLUC-GhNRT2.1e and cLUC-GhNAR2.1 constructs. The *Agrobacterium* inoculum
213   containing the constructs was mixed in equal amounts and injected into the tobacco (Xie et al.,
214   2020). Tobacco was grown under dark conditions for 24 hours, followed by two days in normal
215   environments. The undersides of the leaves were coated with 1 mM Luciferin sodium salt, and
216   after 10 minutes of dark treatment, fluorescent pictures were obtained with a CCD imaging
217   device (Li et al., 2021).

218   # Results

219   **Identification of *NRT2* genes in cotton**
220   We identified 14, 14, 7, and 7 proteins in *G. hirsutum*, *G. barbadense*, *G. raimondii*, and *G.
221   arboreum* using seven AtNRT2 proteins as query sequences, which were named according their
222   homologs in *A. thaliana*. We further analyzed the physicochemical properties of NRT2 proteins
223   (Table S2). In *G. hirsutum*, the protein lengths ranged from 341aa (GhNRT2.1f) to 542aa
224   (GhNRT2.4a and GhNRT2.4b). The isoelectric point ranged from 8.04 (GhNRT2.7a) to 9.51
225   (GhNRT2.1b), indicating that all GhNRT2 proteins are basic proteins. The subcellular
226   localization of most GhNRT2 proteins was predicted at the plasma membrane, while
227   GhNRT2.7a and GhNRT2.7b were localized in the vacuole. The difference in subcellular
228   localization results suggested that GhNRT2 proteins may perform transport functions at different
229   locations. The GhNRT2 proteins have 7 to 12 transmembrane helices, further supporting the
230   predicted subcellular localization results.
231   **Phylogenetic analysis of NRT2 proteins in cotton**
232   The phylogenetic tree of NRT2 proteins was constructed by the NJ method in MEGA7.0
233   software (Fig. 1). The *NRT2* genes were divided into four groups, named Group1 to Group4.
234   Group 1 consisted of *GhNRT2.1s*, *GhNRT2.4s*, and their homologous genes. Group 2 was
235   composed of *GhNRT2.3s* and their homologous genes. *GhNRT2.7s* and their homologs were
236   located in group 3. *GhNRT2.5s* and their homologs were found in group 4. *AtNRT2.2* and
237   *AtNRT2.6* were located in groups 1 and 2, respectively, but their homologous genes were not
238   identified in cotton. The NRT2 proteins of the *At* subgenome of allotetraploid cotton share high
239   homology with those from *G. arboreum*. The NRT2 proteins of the *Dt* subgenome share a high

240   degree of homology with those of *G. raimondii*. The results further verified that the allotetraploid

241   cotton was produced by recombining two diploid species of cotton.

Chromosomal location of *GhNRT2* genes

243   The distribution of *GhNRT2* genes on chromosomes was mapped through gene location

244   information (Fig. 2). In *G. hirsutum*, fourteen *GhNRT2* genes were distributed on twelve

245   chromosomes. Such as chromosomes A05, A07, A08, A09, A12, D05, D07, D08, D09, and D12

246   each contained one *GhNRT2* gene, while chromosomes A03 and D03 each contained two genes.

Gene duplication and synteny analysis of *NRT2* gene in cotton

248   We performed gene duplication and syntenic relationship analysis in *NRT2* genes and identified

249   two tandem repeats in *G. hirsutum*, *GhNRT2.1a/ GhNRT2.3a* and *GhNRT2.1b/ GhNRT2.3b*. In

250   addition, we identified 22 segmental duplications and 119 WGD for the *GhNRT2* genes (Table

251   S3). Synteny analysis revealed a high collinearity relationship between *NRT2* genes. We

252   identified 22, 56, 30, 39, 36, 29, and 27 paralogous or orthologous gene pairs from seven

253   combinations (Gh-Gh, Gh-Gb, Gb-Gb, Gb-Gr, Gh-Gr, Gb-Ga, and Gh-Ga), respectively (Fig. 3).

254   In addition, only *GhNRT2.7a/GbNRT2.7a* had a Ka/Ks ratio >1, indicating that positive selection

255   was experienced. In contrast, the Ka/Ks of other gene pairs were <1, demonstrating that almost

256   all *NRT2* genes underwent purifying selection (Table S4).

Gene structure and conserved motif of *GhNRT2* genes

258   To further study the structural diversity of *GhNRT2* genes, we analyzed their exon-intron

259   structure. Structural analysis of *GhNRT2* genes revealed that *GhNRT2.1s* and *GhNRT2.4s*

260   contained three exons and two introns, while *GhNRT2.3s*, *GhNRT2.5s*, and *GhNRT2.7s* all

261   contained only two exons and one intron (Fig. 4C). Furthermore, we found that genes in the

262   same group have similar structures, probably because the *GhNRT2* genes are highly conserved in

263   structure. The analysis of the gene structure also provided additional evidence for the

264   evolutionary relationship of *NRT2* genes. We identified conserved motifs in GhNRT2 proteins

265   by MEME. We found that almost all GhNRT2 proteins have motifs 1, 2, 3, 4, 5, 6, 7, 8, and 10,

266   suggesting that these proteins are highly conserved and have similar functions. GhNRT2.7a and

267   GhNRT2.7b did not contain motif 9, and GhNRT2.1f was missing in motifs 7, 8, 9, and 10, so

268   we speculated that these proteins might have specific functions (Fig. 4B). To verify the sequence

269   characteristics of GhNRT2 proteins, we performed multiple sequence alignments of GhNRT2

270   protein sequences by DNAMAN (Fig. 4D). All GhNRT2 proteins contained MFS and NNP

271   motifs, demonstrating that they belong to the MFS and NNP families.

Cis-acting element analysis of *GhNRT2* genes

273   The promoter cis-acting elements of *GhNRT2* genes were examined by PlantCARE software to

274   elucidate potential regulatory mechanisms (Fig. 5). We classified the examined cis-acting

275   elements into three categories based on their biological functions (Table S5). The first category

276   was phytohormone-related elements, of which MeJA, GA, auxin, SA, and ABA contained 30, 18,

277   10, 9, and 27, respectively. The second category was stress response elements. We found the

278   highest number of anaerobic induction elements with 34. There was only one anoxic specific

279   inducibility element, and it was present in the promoter region of *GhNRT2.3b*. The third category

280   was growth-related elements. The number of meristem expression elements was the most

281   abundant, containing seven. Based on the results, it is hypothesized that *GhNRT2* genes may

282   participate in plant growth, phytohormone regulation, and abiotic stress.

283   **Tissue-specific expression pattern analysis of *GhNRT2* genes**

284   The tissue expression pattern of *GhNRT2* genes were revealed using RNA-seq data (accession

285   number: PRJNA490626) (Fig. 6). We found that the expression levels of *GhNRT2.1f*,

286   *GhNRT2.3a*, and *GhNRT2.4a* were not detected in all tissues (FPKM<1). The expression levels

287   of *GhNRT2.1a-e* were extremely high in roots. *GhNRT2.3b* and *GhNRT2.4b* were expressed only

288   in the roots, but their expression levels were low. *GhNRT2.5a* and *GhNRT2.5b* had high

289   expression levels in several tissues, with *GhNRT2.5a* primarily expressed in epicalyx, root, and

290   leaf, and *GhNRT2.5b* had high levels in petal, pistil, and sepal. The expression levels of

291   *GhNRT2.7a* and *GhNRT2.7b* were higher in leaves and ovules. To validate the RNA-seq results,

292   we analyzed the expression patterns of *GhNRT2* genes in root, stem, and leaf by qRT-PCR (Fig.

293   7). We designed specific primers for each *GhNRT2* gene to detect accurate gene expression

294   levels. We found similar results of qRT-PCR and RNA-seq analysis, further validating the

295   expression profile of *GhNRT2* genes. The *GhNRT2* genes were highly expressed in roots,

296   suggesting that they may function in nitrate uptake. The qRT-PCR assay showed that

297   *GhNRT2.5a* and *GhNRT2.5b* had the highest expression in roots. Combining the results of RNA-

298   seq and qRT-PCR, we found that *GhNRT2.5a* and *GhNRT2.5b* may be expressed in roots and

299   aerial parts, and their expression patterns were similar to those of *AtNRT2.5* (Lezhneva et al.,

300   2014). *GhNRT2.7a* and *GhNRT2.7b* showed high expression in leaves and ovules, and they may

301   have potential functions in nitrate storage.

302   **Expression patterns of *GhNRT2* genes at low nitrate concentrations**

303   After one week of nitrogen-free treatment, cotton seedlings were resupplied with 0.25mM NO_3^-

304   to investigate the expression pattern of *GhNRT2* genes at low nitrate concentrations. We found

305   that *GhNRT2.7a* and *GhNRT2.7b* were barely expressed in the roots by tissue-specific analysis.

306   Therefore, we selected nine *GhNRT2* genes with high or specific expression in the roots and

307   analyzed their expression levels at low nitrate concentrations by qRT-PCR (Fig. 8). The *GhNRT2*

308   genes exhibited different expression levels after NO_3^- resupply. Interestingly, only the

309   *GhNRT2.1(a-e)* genes were significantly up-regulated and peaked at 3 or 6 hours before

310   gradually decreasing. However, the expression levels of *GhNRT2.4b*, *GhNRT2.5a* and

311   *GhNRT2.5b* genes were reduced after NO_3^- resupply, and the reduction was more pronounced for

312   *GhNRT2.5a* and *GhNRT2.5b*. *GhNRT2.3b* may not be sensitive to nitrate resupply and is weakly

313   upregulated. It may be because the GhNRT2.1(a-e) proteins belong to the inducible high-affinity

314   transport system (iHATS) which is induced by nitrate supply. In contrast, GhNRT2.4b,

315   GhNRT2.5a and GhNRT2.5b proteins belong to constitutive high-affinity transport systems

316   (cHATS), which are active in plants not supplied with nitrate (Lezhneva et al., 2014). The

317   *GhNRT2.1e* showed the most significant up-regulation of all genes, and its expression level

318   reached the highest at 6h, which was about 180-fold increase compared to 0h. *GhNRT2.1e* may

319   be a critical gene to promote the absorption and transport of nitrate in cotton.

320   **Phenotypic, physiological, and biochemical evaluation of *GhNRT2.1e*-overexpressed**

321   ***Arabidopsis* plants**

322   To elucidate the function of *GhNRT2.1e*, we cloned the coding sequence of *GhNRT2.1e* into the
323   pRI101 vector containing the Cauliflower mosaic virus 35S promoter, and overexpressed it in
324   *Arabidopsis*. We extracted RNA and genomic DNA from T2 generation of overexpressed lines
325   and analyzed the expression level of *GhNRT2.1e* under a normal nitrate environment by qRT-
326   PCR and PCR (Fig. 9B and Fig. S1). Results indicated that *GhNRT2.1e* had been successfully
327   transferred into *Arabidopsis* and could be stably expressed. Three T3 generation overexpressed
328   lines were screened for further functional studies of *GhNRT2.1e*. Plants were supplied with 0.25
329   mM and 2.5 mM of nitrate to create a nitrogen deficiency and normal supply. After six weeks of
330   growth, plants were evaluated for phenotypic, physiological, and biochemical traits. There were
331   no phenotypic differences between overexpressed lines and WT under 2.5 mM nitrate conditions.
332   However, the overexpressed lines exhibited better growth than the WT when watered with 0.25
333   mM NO_3^- (Fig. 9A). We further measured dry weight to reflect differences between plants and
334   found that the overexpressed lines had higher biomass than WT (Fig. 9C). To reflect
335   physiological differences between plants, we measured nitrogen and nitrate content (Fig. 9D, E).
336   There were no differences between plants under normal conditions, but overexpressed lines had
337   higher levels of nitrogen and nitrate at low nitrate concentrations. Additionally, we found that
338   nitrogen accumulation in overexpressed lines was increased under low nitrate conditions (Fig.
339   10A). We also calculated the NUpE and NUtE of plants and found that the NUpE and NUtE
340   were higher in the overexpressed lines (Fig. 10B, C). We speculated that the overexpressed lines
341   may promote nitrate uptake, allowing plants to accumulate and utilize more nitrogen and nitrate.
342   To further analyze nitrate uptake and utilization in plants, we measured nitrogen-metabolizing
343   enzyme activity (Fig. 10D-F). Nitrogen-metabolizing enzyme activity was higher in the
344   overexpressed lines at low nitrate concentrations, but there were no apparent differences at
345   normal concentrations. We also observed higher amino acid contents in overexpressed lines (Fig.
346   10G). In conclusion, *Arabidopsis* undergoes low-affinity transport under normal conditions, and
347   *GhNRT2.1e* plays a minor role, so there is no apparent difference between overexpressed
348   *Arabidopsis* and WT. In contrast, under low nitrate conditions, *GhNRT2.1e* plays an essential
349   role as a high-affinity transporter protein to absorb more nitrate into nitrogen metabolism, which
350   produces more nitrogen assimilation products for plant growth with the action of nitrogen
351   metabolizing enzymes.
352   **Evaluation of morphology, physiological indexes, and biochemical characters of**
353   ***GhNRT2.1e*-silenced plants**
354   To further elucidate the function of *GhNRT2.1e*, we selected the TRV vector for the VIGS assay.
355   To verify the effectiveness of the vector, we injected TRV2:PDS into cotton leaves. Cotton
356   leaves showed an albino phenotype after 14 days TRV2:PDS injection, indicating that the vector
357   used was effective (Fig. 11A). After injection, plants were given nutrient solutions with a nitrate
358   concentration of 2.5 mM and 0.25 mM to create normal and low nitrate environments,
359   respectively. To evaluate gene silencing efficiency, we determined the expression levels of
360   *GhNRT2.1e* in WT, TRV2:00, and TRV2:GhNRT2.1e plants by qRT-PCR after two weeks of
361   plant growth (Fig. 11C). The expression levels of the *GhNRT2.1e* gene were not significantly
362   different in WT and TRV2:00, indicating that the injection of an empty vector did not affect the

363 plants. However, the expression level of the *GhNRT2.1e* gene was significantly down-regulated
364 in TRV2:GhNRT2.1e plants compared with WT and TRV2:00, which indicated that gene
365 silencing was successful. After four weeks of growth, there were no apparent differences
366 between plants under 2.5 mM nitrate conditions. However, silenced plants showed dwarf and
367 slow growth under low nitrate conditions compared to WT and TRV2:00 (Fig. 11B). To further
368 analyze the morphological differences between VIGS and control plants, we evaluated
369 physiological traits including dry weight, nitrogen content, and nitrate content (Fig. 11D-F). In
370 the low nitrate environment, VIGS plants had lower dry weight, nitrogen, and nitrate content
371 than WT and TRV2:00. We further analyzed NUpE and NUtE and found that the uptake and
372 utilization efficiencies of VIGS plants were low as compared to WT and TRV2:00 (Fig. 12A, B).
373 Additionally, we also found lower total nitrogen accumulation in VIGS plants (Fig. 12C). The
374 differences exhibited by the plants in normal and low nitrate environments could be due to the
375 high nitrate concentration in the normal environment, where plants mainly undergo low-affinity
376 transport. However, GhNRT2.1e is a high-affinity transporter protein that may not function or
377 have less effect in environments with high nitrate concentrations. In low nitrate environments,
378 plants mainly undergo high-affinity transport, and *GhNRT2.1e* plays an essential role as a critical
379 gene. Therefore, nitrate uptake by *GhNRT2.1e* silenced plants is inhibited, which affects the
380 accumulation of nitrogen and nitrate and ultimately reduces plant biomass. We also found that
381 chlorophyll content decreased in VIGS plants under low nitrate conditions (Fig. 12D). Nitrogen
382 is a vital chlorophyll component, essential for photosynthesis and plant growth. Therefore,
383 reducing chlorophyll content also reflects the inhibition of nitrogen uptake and utilization by
384 VIGS plants. We measured nitrogen metabolizing enzyme activity to reflect whether nitrate
385 uptake by silenced plants was affected (Fig. 12E-G). The activity of nitrogen metabolizing
386 enzymes was reduced in VIGS plants compared with controls. We also observed that the amino
387 acid content was reduced in VIGS plants (Fig. 12H). These results suggested that silencing of
388 *GhNRT2.1e* affects nitrate uptake by plants, thereby reducing nitrogen-metabolizing enzyme
389 activity and amino acid content. We assessed the concentrations of oxidants and antioxidant
390 enzymes in plants including CAT, POD, SOD, and MDA (Fig. 12I-L). Under low nitrate
391 conditions, the concentrations of CAT, POD, and SOD in VIGS plants decreased, and the
392 concentration of MDA increased compared with control plants. Under stress conditions, elevated
393 levels of ROS lead to membrane damage and an increase in MDA levels. High concentrations of
394 MDA in silenced plants indicated increased peroxidation of plant cells and oxidative damage to
395 the plants, as further showed by reduced antioxidant enzyme activity. These results showed that
396 plants suffer from nutrient stress in low nitrate environments, and GhNRT2.1e perform high-
397 affinity transport to maintain a partial nitrate supply. However, silencing of *GhNRT2.1e* resulted
398 inhibition of nitrate uptake and reduced tolerance to low-nitrate environments, leading to
399 oxidative damage in plants.
400 **GhNRT2.1e interacts with GhNAR2.1**
401 We performed a yeast two-hybrid assay to verify interaction between GhNRT2.1e and
402 GhNAR2.1 in cotton as we identified the homologous gene GhNAR2.1 of AtNAR2.1 in
403 *G.hirsutum*. On SD-LW medium, yeast carrying pPR3-N-GhNRT2.1e/pBT3-C-GhNAR2.1,

404 pPR3-N-GhNRT2.1e/pBT3-C, and pPR3-N/pBT3-C-GhNAR2.1 could grow normally (Fig.
405 13A). On the SD-AHLW medium, only yeast carrying pPR3-N-GhNRT2.1e/pBT3-C-
406 GhNAR2.1 could grow normally (Fig. 13B). Among them, pPR3-N and pBT3-C were empty
407 vectors, and the constructs pBT3-C-GhNAR2.1 and pPR3-N-GhNRT2.1e were connected with
408 empty vectors as negative controls. The results indicated that GhNRT2.1e interacts with
409 GhNAR2.1, which was further verified by LCI assay. SPL3-nLUC and FHY3-cLUC served as
410 positive controls (Fig. 13C). In tobacco leaves, only GhNRT2.1e-nLUC/GhNAR2.1-cLUC could
411 fluoresce (Fig. 13D). The results showed that GhNRT2.1e and GhNAR2.1 could also interact in
412 vivo.

Discussion

Identification and characterization of the *NRT2* genes

415 Nitrogen fertilizer can promote cotton growth but over-application of nitrogen fertilizer causes
416 waste of resources and environmental pollution. Therefore, it is necessary to apply nitrogen
417 fertilizer rationally and improve the NUE to save resources and protect the environment (Xu et
418 al., 2012). We can explore key genes regulating nitrogen uptake and utilization through
419 molecular methods and breeding new cotton cultivars to improve NUE. NRT2 proteins have
420 been found in plants, which can uptake and transport nitrate at low nitrate concentrations and are
421 particularly important for increasing NUE (Chen et al., 2016).
422 In this research, the numbers *NRT2* genes were twice in tetraploid cotton as in diploid
423 cotton species, verifying that *G. hirsutum* was developed by crossing two diploid cotton species
424 (Huang et al., 2020). Gene duplication promotes functional differentiation, improves adaptation
425 to the environment during evolution, and expands the gene family (Cannon et al., 2004). In the
426 replication analysis of *NRT2* genes, segmental duplication, tandem repeats, and WGD were
427 observed to expand the *NRT2* gene family. Besides, the *NRT2* genes may have diverged during
428 the duplication process to generate new functions. Almost all *NRT2* genes have undergone
429 purifying selection during evolution. Similar results were observed for changes in the number of
430 NRT2 proteins in *Brassica* families (Tong et al., 2020). Purification selection is essential to
431 reduce deleterious mutations in the *NRT2* genes and increase their stability. We performed
432 subcellular localization predictions and found that most of the cotton NRT2 proteins were
433 present in the plasma membrane, and only NRT2.7 was on the vacuolar membrane. These results
434 are similar to the localization of *Arabidopsis* NRT2 proteins (Lezhneva et al., 2014).
435 Furthermore, our prediction of the transmembrane helix of NRT2 proteins confirmed their
436 localization to membranes. The plasma membrane controls the inflow and outflow of substances
437 during the exchange of ions, metabolites, and nutrients (Barberon et al., 2014). Therefore, NRT2
438 proteins on membranes are essential for cellular uptake and transport of nitrate. Predicting cis-
439 acting elements helps us speculate on gene function (Feng et al., 2021). Some hormone-related
440 elements were found in the promoter region of *GhNRT2* genes. Among those, ABA, auxin, and
441 cytokinin are closely related to regulating nitrogen signaling and nitrogen uptake (Kiba et al.,
442 2011). Nitrate controls ABA accumulation in root tips, while ABA regulates lateral root
443 formation by nitrate (Ondzighi-Assoume et al., 2016). *Arabidopsis* can regulate auxin levels in

444 their roots according to their nitrogen status (Kiba et al., 2011). In watermelon, SA regulates
445 nitrate uptake and assimilation (Vega et al., 2019). The expression of *GhNRT2* genes in roots and
446 their response to low nitrate may be related to ABA, auxin, and SA response elements and
447 phytohormone regulation of nitrogen signaling.

448 **Expression analysis of the *GhNRT2* genes**

449 Tissue differential expression analysis facilitates the investigation of gene functions (Yang et al.,
450 2019). We identified differential expression of *GhNRT2* genes by RNA-seq and qRT-PCR (Fig.
451 6, 7). The *GhNRT2* genes were expressed in roots, which might be related to nitrate uptake by
452 the roots. Both *GhNRT2.5a* and *GhNRT2.5b* had the high expression in several tissues and may
453 be implicated in root uptake and inter-tissue transport. *GhNRT2.7a* and *GhNRT2.7b* were
454 expressed mainly in ovules and leaves and may participate in nitrate storage and accumulation.
455 There was a similar expression in *Arabidopsis*, where *AtNRT2.7* was expressed in leaves and
456 seeds, while other genes were expressed in roots (Orsel et al., 2002). Similar situations were
457 identified in cassava and rapeseed (Du RJ et al., 2022; You et al., 2022). The similarity in the
458 expression of homologous genes in different species suggests that *NRT2* genes are relatively
459 conserved during evolution and have an essential role in plants. The tissue specificity of
460 *GhNRT2* genes suggested that they function at different sites to jointly promote nitrate uptake,
461 transport, storage, and utilization.

462   The expression levels of *GhNRT2* genes were investigated after nitrate supplementation.
463 The *GhNRT2.1(a-e)* genes were strongly induced by nitrate, whereas *GhNRT2.4b*, *GhNRT2.5a*
464 and *GhNRT2.5b* were significantly repressed (Fig. 8). The cHATS is active without nitrate
465 supply and can initiate nitrate-induced genes (Kiba et al., 2012). In lack of nitrate supply, iHATS
466 is barely expressed, whereas expression is high hours of nitrate induction (Kiba et al., 2012;
467 Orsel et al., 2002). In *A. thaliana*, iHATS activity is mainly dependent on *AtNRT2.1* (Li et al.,
468 2007). In contrast, *AtNRT2.4* and *AtNRT2.5* belong to cHATS and are expressed under very low
469 nitrate environment or nitrogen starvation conditions (Kotur & Glass, 2015). Therefore, we
470 speculated that the GhNRT2.1(a-e) proteins might belong to iHATS and the GhNRT2.4b,
471 GhNRT2.5a and GhNRT2.5b proteins belong to cHATS. Although they perform different
472 functions, their interactions are necessary for the growth of plants under a restricted nitrogen
473 supply. In addition, the expression of *GhNRT2.1(a-e)* genes first increased and then decreased,
474 which was consistent with *CsNRT2* (Li et al., 2018). Thus, we speculated that plant nitrogen
475 requirements may regulate the expression of *NRT2* genes and that many plants have similar
476 conditions. In cassava, *MeNRT2.2* was strongly induced in nitrate deficiency (You et al., 2022).
477 In barley*, HvNRT2* genes also have a similar expression (Guo et al., 2020).

478 **The potential role of *GhNRT2.1e* in increasing NUE**

479 *GhNRT2.1e* was the most up-regulated gene at low nitrate concentration and may be a key gene
480 regulating nitrate uptake and transport. We validated the function of *GhNRT2.1e* using
481 overexpression in *A. thaliana* and silencing in *G. hirsutum*. As transgenic cotton takes longer, but
482 *Arabidopsis* is a convenient model plant to study gene function, we investigated the role of
483 *GhNRT2.1e* by heterologous expression in *Arabidopsis* (Xiao et al., 2022). The *NRT2* genes were
484 overexpressed and can promote nitrate uptake and transport, and increase plant biomass. The

485   cassava *MeNRT2.2* gene was overexpressed and increased the fresh weight of transgenic

486   *Arabidopsis* (You et al., 2022). The study of the *NRT2* genes in chrysanthemum demonstrated

487   that nitrate uptake was increased when *CmNRT2.4* was used in transgenic *Arabidopsis* and that

488   overexpression of *CmNRT2.1* also contributed to the uptake of nitrate (Gu et al., 2016). The

489   *HvNRT2.1* gene was overexpressed and increased nitrate and nitrogen content (Guo et al., 2020).

490   The *CsNRT2.4* gene was overexpressed, increasing biomass and promoting lateral root

491   development (Zhang et al., 2021). The results of this study demonstrated that in the presence of

492   low nitrate supply levels, transgenic *Arabidopsis* promotes nitrate uptake, increasing nitrate and

493   nitrogen accumulation and ultimately contributing to biomass accumulation (Fig. 9, 10).

494   Therefore, *GhNRT2.1e* promotes nitrate uptake and transport, resulting in the better growth

495   potential of transgenic *Arabidopsis* under limited nitrate conditions. The current research results

496   on *Arabidopsis* overexpression lines will provide some reference for future research on

497   transgenic cotton.

498   VIGS is often used to assess the function of genes, which can inhibit gene expression (Gao

499   et al., 2011). This study revealed no significant difference between *GhNRT2.1e*-silenced plants

500   and control at normal nitrate concentrations. At low nitrate concentrations, *GhNRT2.1e*-silenced

501   plants had lower dry weight, nitrogen and nitrate accumulation, chlorophyll content, and nitrogen

502   uptake and use efficiency than control plants (Fig. 11, 12). Similar results were obtained by

503   knocking out or silencing the *NRT2* gene in other plants. For example, HATS activity was

504   significantly reduced in AtNRT2.1-deficient mutants (Filleur et al., 2001). In cucumber,

505   knockdown of *CsNRT2.1* also inhibited nitrate uptake (Li et al., 2018). We speculate that

506   silencing of *GhNRT2.1e* affects nitrate uptake by VIGS plants, thereby inhibiting nitrate and

507   nitrogen utilization and accumulation. The reduced nitrogen supply to stems and leaves affects

508   plant photosynthesis and biomass accumulation. Therefore, the *GhNRT2.1e* gene increased

509   nitrate uptake and transport and promoted cotton growth at low nitrate concentrations.

510   Previous studies of *Arabidopsis* and rice nitrate transporter Km data demonstrated that

511   nitrogen transporters regulate the activities of nitrogen-metabolizing enzymes (Glass et al.,

512   2002). Nitrogen absorbed by transporters is converted into amino acids by metabolic enzymes

513   (Iqbal et al., 2020b). Therefore, the activity of the nitrate transporter can be judged by measuring

514   metabolic enzyme activity and amino acid content. We found that nitrogen metabolizing enzyme

515   activity and amino acid content were higher in transgenic *Arabidopsis* (Fig. 10). However,

516   nitrogen metabolizing enzyme activity and amino acid content were found to be lower in

517   *GhNRT2.1e*-silenced plants (Fig. 12). It might be due to the silencing of the *GhNRT2.1e* gene

518   that inhibits nitrate absorption by VIGS plants and reduces the NO_3^- that enters the assimilation

519   process, thereby affecting the assimilation process and reducing metabolic enzyme activity and

520   amino acid content. However, transgenic *Arabidopsis* can absorb more NO_3^- and promote the

521   metabolic process, so metabolic enzyme activity and amino acid content are increased. Previous

522   studies on other nitrogen-related genes had similar results. The *CPSF30* promoted nitrate

523   signaling, while NR activity and amino acid content were reduced in mutants (Hou et al., 2021).

524   *BnaA2.Gln1;4* was expressed in root and shoot with a high affinity for nitrogen and

525   *BnaA2.Gln1;4* overexpression increased GS and GOGAT activity (Zhou et al., 2022). *FIP1* can

526 regulate nitrate uptake and transport, and nitrogen-metabolizing enzyme activity and nitrate
527 content were reduced in *fip1* mutants (Wang et al., 2018).
528   When stressed, plants generate excessive reactive oxygen species (ROS), and cells are
529 damaged by oxidation, which may result in plant death (Caverzan et al., 2016). MDA is a
530 product of lipid breakdown, and the degree of peroxidation in plant cells can be measured by
531 detecting MDA content (Wang et al., 2018). Antioxidant enzymes function in maintaining the
532 homeostasis of plant organelles (Hasanuzzaman et al., 2020). In this research, the oxidant and
533 antioxidant enzyme activities were similar between *GhNRT2.1e*-silenced plants and controls at
534 normal nitrate concentrations. However, at low nitrate concentrations, VIGS plants had higher
535 MDA concentrations and lower activities of SOD, POD, and CAT than control plants (Fig. 12).
536 Similar results were found in other studies that *GhNPL5* enhanced plant tolerance under
537 nitrogen-limiting conditions but also showed lower antioxidant enzyme activity and higher
538 oxidant content in VIGS plants (Magwanga et al., 2019). It may be because the production and
539 elimination of ROS are in a dynamic equilibrium in plants at normal nitrate concentrations so
540 that they do not cause damage to plant cells. Plants are subjected to abiotic stress at low nitrate
541 concentrations, but *GhNRT2* genes can carry out high-affinity nitrate transport, maintain partial
542 nitrogen supply, and reduce plant oxidative damage. The results indicated that *GhNRT2.1e* could
543 improve cotton tolerance under low nitrogen conditions.
544   Interactions between proteins provide essential information for characterizing cells'
545 biological activities and metabolic processes (Mehari et al., 2021). NAR2 is a chaperone protein
546 and has been identified in many plants. All AtNRT2 proteins can interact with AtNAR2.1 except
547 AtNRT2.7 (Kotur et al., 2012). AtNRT2.5 interacts with AtNAR2.1 to create a 150 kDa complex
548 in plasma membrane to facilitate nitrate transport (Kotur & Glass, 2015). In rice, OsNRT2.1,
549 OsNRT2.2, and OsNRT2.3a were demonstrated to interact with OsNAR2.1 by yeast two-hybrid
550 experiments (Yan et al., 2011). In chrysanthemum, the interaction of CmNRT2.1 and CmNAR2
551 in vivo was confirmed by yeast two-hybrid and BiFC assays (Gu et al., 2016). In this research,
552 we demonstrated that GhNRT2.1e interacts with GhNAR2.1 using yeast two-hybrid and LCI
553 assays (Fig. 13). We speculated that GhNRT2.1e and GhNAR2.1 can also form a complex in the
554 plasma membrane, and the interaction promotes nitrate uptake and transport.

Conclusions

556 In this work, genome-wide identification and functional characterization of *GhNRT2* genes in *G.*
557 *hirsutum* was performed. Most NRT2 proteins were predicted at the plasma membrane. The
558 results of phylogeny, gene structure, and conserved motifs indicated that GhNRT2 proteins were
559 conserved during evolution. Most *GhNRT2* genes were found expressed in roots by RNA-seq
560 and qRT-PCR. When 0.25mM nitrate was resupplied, the *GhNRT2* genes showed different
561 expression patterns. *GhNRT2.1e* was the most highly up-regulated and essential gene involved in
562 nitrate uptake at low concentrations. We performed functional validation of *GhNRT2.1e* using
563 overexpression in *A. thaliana* and silencing in *G. hirsutum*. *Arabidopsis* plants overexpressing
564 *GhNRT2.1e* exhibited increased biomass, nitrogen and nitrate accumulation, nitrogen uptake and
565 utilization efficiency, nitrogen-metabolizing enzyme activity, and amino acid content at low

nitrate concentrations. VIGS plants exhibited reduced biomass, chlorophyll content, nitrogen and nitrate accumulation, nitrogen uptake and use efficiency, nitrogen-metabolizing enzyme activity, amino acid content, and tolerance under low nitrate conditions. These results demonstrated that *GhNRT2.1e* promoted nitrate uptake, regulation of nitrogen metabolism, and biomass accumulation. We demonstrated the interaction of GhNRT2.1e with GhNAR2.1 by yeast two-hybrid and LCI assays and speculated that they work together to promote nitrate transport. This study illustrates the function of *GhNRT2* genes and provides new ideas for improving NUE, increasing yield, and developing new varieties with high nitrogen utilization.

References

Akbudak MA, Filiz E, Çetin D. 2022. Genome-wide identification and characterization of high-affinity nitrate transporter 2 (NRT2) gene family in tomato (Solanum lycopersicum) and their transcriptional responses to drought and salinity stresses. *Journal of Plant Physiology* 272:153684 DOI: 10.1016/j.jplph.2022.153684.

Amarasinghe BH, de Bruxelles GL, Braddon M, Onyeocha I, Forde BG, Udvardi MK. 1998. Regulation of GmNRT2 expression and nitrate transport activity in roots of soybean (Glycine max). *Planta* 206:44-52 DOI: 10.1007/s004250050372.

Bailey TL, Johnson J, Grant CE, Noble WS. 2015. The MEME Suite. *Nucleic Acids Research* 43:W39-W49 DOI: 10.1093/nar/gkv416.

Barberon M, Dubeaux G, Kolb C, Isono E, Zelazny E, Vert G. 2014. Polarization of IRON-REGULATED TRANSPORTER 1 (IRT1) to the plant-soil interface plays crucial role in metal homeostasis. *Proceedings of the National Academy of Sciences of the United States of America* 111:8293-8298 DOI: 10.1073/pnas.1402262111.

Berardini TZ, Reiser L, Li D, Mezheritsky Y, Muller R, Strait E, Huala E. 2015. The Arabidopsis information resource: Making and mining the "gold standard" annotated reference plant genome. *Genesis* 53:474-485 DOI: 10.1002/dvg.22877.

Cai C, Wang JY, Zhu YG, Shen QR, Li B, Tong YP, Li ZS. 2008. Gene structure and expression of the high-affinity nitrate transport system in rice roots. *Journal of Integrative Plant Biology* 50:443-451 DOI: 10.1111/j.1744-7909.2008.00642.x.

Cannon SB, Mitra A, Baumgarten A, Young ND, May G. 2004. The roles of segmental and tandem gene duplication in the evolution of large gene families in Arabidopsis thaliana. *BMC Plant Biology* 4:10 DOI: 10.1186/1471-2229-4-10.

Caverzan A, Casassola A, Brammer SP. 2016. Antioxidant responses of wheat plants under stress. *Genetics and Molecular Biology* 39:1-6 DOI: 10.1590/1678-4685-GMB-2015-0109.

Chen C, Chen H, Zhang Y, Thomas HR, Frank MH, He Y, Xia R. 2020. TBtools: An Integrative Toolkit Developed for Interactive Analyses of Big Biological Data. *Molecular Plant* 13:1194-1202 DOI: 10.1016/j.molp.2020.06.009.

Chen J, Zhang Y, Tan Y, Zhang M, Zhu L, Xu G, Fan X. 2016. Agronomic nitrogen-use efficiency of rice can be increased by driving OsNRT2.1 expression with the OsNAR2.1 promoter. *PLANT Biotechnology Journal* 14:1705-1715 DOI: 10.1111/pbi.12531.

605 Chopin F, Orsel M, Dorbe MF, Chardon F, Truong HN, Miller AJ, Krapp A, Daniel-Vedele F.
606   2007. The Arabidopsis ATNRT2.7 nitrate transporter controls nitrate content in seeds. *The*
607   *Plant Cell* 19:1590-1602 DOI: 10.1105/tpc.107.050542.
608 Clough SJ, Bent AF. 1998. Floral dip: a simplified method for Agrobacterium-mediated
609   transformation of Arabidopsis thaliana. *The Plant Journal* 16:735-743 DOI: 10.1046/j.1365-
610   313x.1998.00343.x.
611 Dechorgnat J, Nguyen CT, Armengaud P, Jossier M, Diatloff E, Filleur S, Daniel-Vedele F.
612   2011. From the soil to the seeds: the long journey of nitrate in plants. *Journal of Eeperimental*
613   *Botany* 62:1349-1359 DOI: 10.1093/jxb/erq409.
614 Du RJ, Wu ZX, Yu ZX, Li PF, Mu JY, Zhou J, Li JN, Du H. 2022. Genome-Wide
615   Characterization of High-Affinity Nitrate Transporter 2 (NRT2) Gene Family in Brassica
616   napus. *International Journal of Molecular Sciences* 23:4965 DOI: 10.3390/ijms23094965.
617 El-Gebali S, Mistry J, Bateman A, Eddy SR, Luciani A, Potter SC, Qureshi M, Richardson LJ,
618   Salazar GA, Smart A, Sonnhammer E, Hirsh L, Paladin L, Piovesan D, Tosatto S, Finn RD.
619   2019. The Pfam protein families database in 2019. *Nucleic Acids Research* 47:D427-D432
620   DOI: 10.1093/nar/gky995.
621 Feng J, Chen Y, Xiao X, Qu Y, Li P, Lu Q, Huang J. 2021. Genome-wide analysis of the CalS
622   gene family in cotton reveals their potential roles in fiber development and responses to stress.
623   *PeerJ* 9:e12557 DOI: 10.7717/peerj.12557.
624 Filleur S, Dorbe MF, Cerezo M, Orsel M, Granier F, Gojon A, Daniel-Vedele F. 2001. An
625   arabidopsis T-DNA mutant affected in Nrt2 genes is impaired in nitrate uptake. *FEBS Letters*
626   489:220-224 DOI: 10.1016/s0014-5793(01)02096-8.
627 Gao X, Britt RJ, Shan L, He P. 2011. Agrobacterium-mediated virus-induced gene silencing
628   assay in cotton. *Journal of Visualized Experiments* 54:2938 DOI: 10.3791/2938.
629 Glass AD, Britto DT, Kaiser BN, Kinghorn JR, Kronzucker HJ, Kumar A, Okamoto M, Rawat
630   S, Siddiqi MY, Unkles SE, Vidmar JJ. 2002. The regulation of nitrate and ammonium
631   transport systems in plants. *Journal of Experimental Botany* 53:855-864 DOI:
632   10.1093/jexbot/53.370.855.
633 Gu C, Song A, Zhang X, Wang H, Li T, Chen Y, Jiang J, Chen F, Chen S. 2016. Cloning of
634   chrysanthemum high-affinity nitrate transporter family (CmNRT2) and characterization of
635   CmNRT2.1. *Scientific Reports* 6:23462 DOI: 10.1038/srep23462.
636 Guo B, Li Y, Wang S, Li D, Lv C, Xu R. 2020. Characterization of the Nitrate Transporter gene
637   family and functional identification of HvNRT2.1 in barley (Hordeum vulgare L.). *PLoS One*
638   15:e232056 DOI: 10.1371/journal.pone.0232056.
639 Hasanuzzaman M, Bhuyan M, Zulfiqar F, Raza A, Mohsin SM, Mahmud JA, Fujita M,
640   Fotopoulos V. 2020. Reactive Oxygen Species and Antioxidant Defense in Plants under
641   Abiotic Stress: Revisiting the Crucial Role of a Universal Defense Regulator. *Antioxidants*
642   *(Basel)* 9:681. DOI: 10.3390/antiox9080681Horton P, Park KJ, Obayashi T, Fujita N, Harada
643   H, Adams-Collier CJ, Nakai K. 2007. WoLF PSORT: protein localization predictor. *Nucleic*
644   *Acids Research* 35:W585-W587 DOI: 10.1093/nar/gkm259.

645 Hou Y, Sun J, Wu B, Gao Y, Nie H, Nie Z, Quan S, Wang Y, Cao X, Li S. 2021. CPSF30-L-
646   mediated recognition of mRNA m(6)A modification controls alternative polyadenylation of
647   nitrate signaling-related gene transcripts in Arabidopsis. *Molecular Plant* 14:688-699 DOI:
648   10.1016/j.molp.2021.01.013.
649 Hu B, Jin J, Guo AY, Zhang H, Luo J, Gao G. 2015. GSDS 2.0: an upgraded gene feature
650   visualization server. *Bioinformatics* 31:1296-1297 DOI: 10.1093/bioinformatics/btu817.
651 Hu Y, Chen J, Fang L, Zhang Z, Ma W, Niu Y, Ju L, Deng J, Zhao T, Lian J, Baruch K, Fang D,
652   Liu X, Ruan YL, Rahman MU, Han J, Wang K, Wang Q, Wu H, Mei G, Zang Y, Han Z, Xu
653   C, Shen W, Yang D, Si Z, Dai F, Zou L, Huang F, Bai Y, Zhang Y, Brodt A, Ben-Hamo H,
654   Zhu X, Zhou B, Guan X, Zhu S, Chen X, Zhang T. 2019. Gossypium barbadense and
655   Gossypium hirsutum genomes provide insights into the origin and evolution of allotetraploid
656   cotton. *Nature Genetics* 51:739-748 DOI: 10.1038/s41588-019-0371-5.
657 Huang G, Wu Z, Percy RG, Bai M, Li Y, Frelichowski JE, Hu J, Wang K, Yu JZ, Zhu Y. 2020.
658   Genome sequence of Gossypium herbaceum and genome updates of Gossypium arboreum and
659   Gossypium hirsutum provide insights into cotton A-genome evolution. *Nature Genetics*
660   52:516-524 DOI: 10.1038/s41588-020-0607-4.
661 Iqbal A, Qiang D, Alamzeb M, Xiangru W, Huiping G, Hengheng Z, Nianchang P, Xiling Z,
662   Meizhen S. 2020b. Untangling the molecular mechanisms and functions of nitrate to improve
663   nitrogen use efficiency. *Journal of the Science of Food and Agriculture* 100:904-914 DOI:
664   10.1002/jsfa.10085.
665 Iqbal A, Qiang D, Zhun W, Xiangru W, Huiping G, Hengheng Z, Nianchang P, Xiling Z,
666   Meizhen S. 2020a. Growth and nitrogen metabolism are associated with nitrogen-use
667   efficiency in cotton genotypes. *Plant Physiology and Biochemistry* 149:61-74 DOI:
668   10.1016/j.plaphy.2020.02.002.
669 Kiba T, Feria-Bourrellier AB, Lafouge F, Lezhneva L, Boutet-Mercey S, Orsel M, Bréhaut V,
670   Miller A, Daniel-Vedele F, Sakakibara H, Krapp A. 2012. The Arabidopsis nitrate transporter
671   NRT2.4 plays a double role in roots and shoots of nitrogen-starved plants. *The Plant Cell*
672   24:245-258 DOI: 10.1105/tpc.111.092221.
673 Kiba T, Kudo T, Kojima M, Sakakibara H. 2011. Hormonal control of nitrogen acquisition: roles
674   of auxin, abscisic acid, and cytokinin. *Journal of Experimental Botany* 62:1399-1409. DOI:
675   10.1093/jxb/erq410Kotur Z, Mackenzie N, Ramesh S, Tyerman SD, Kaiser BN, Glass A.
676   2012. Nitrate transport capacity of the Arabidopsis thaliana NRT2 family members and their
677   interactions with AtNAR2.1. *New Phytologist* 194:724-731 DOI: 10.1111/j.1469-
678   8137.2012.04094.x.
679 Kotur Z, Glass AD. 2015. A 150 kDa plasma membrane complex of AtNRT2.5 and AtNAR2.1 is
680   the major contributor to constitutive high-affinity nitrate influx in Arabidopsis thaliana. *Plant
681   Cell and Environment* 38:1490-1502 DOI: 10.1111/pce.12496.
682 Krogh A, Larsson B, von Heijne G, Sonnhammer EL. 2001. Predicting transmembrane protein
683   topology with a hidden Markov model: application to complete genomes. *Journal of
684   Molecular Biology* 305:567-580 DOI: 10.1006/jmbi.2000.4315.

685   Kumar S, Stecher G, Tamura K. 2016. MEGA7: Molecular Evolutionary Genetics Analysis

686   Version 7.0 for Bigger Datasets. *Molecular Biology and Evolution* 33:1870-1874 DOI:

687   10.1093/molbev/msw054.

688   Larkin MA, Blackshields G, Brown NP, Chenna R, McGettigan PA, McWilliam H, Valentin F,

689   Wallace IM, Wilm A, Lopez R, Thompson JD, Gibson TJ, Higgins DG. 2007. Clustal W and

690   Clustal X version 2.0. *Bioinformatics* 23:2947-2948 DOI: 10.1093/bioinformatics/btm404.

691   Léran S, Varala K, Boyer JC, Chiurazzi M, Crawford N, Daniel-Vedele F, David L, Dickstein R,

692   Fernandez E, Forde B, Gassmann W, Geiger D, Gojon A, Gong JM, Halkier BA, Harris JM,

693   Hedrich R, Limami AM, Rentsch D, Seo M, Tsay YF, Zhang M, Coruzzi G, Lacombe B.

694   2014. A unified nomenclature of NITRATE TRANSPORTER 1/PEPTIDE TRANSPORTER

695   family members in plants. *Trends in Plant Science* 19:5-9 DOI: 10.1016/j.tplants.2013.08.008.

696   Lescot M, Déhais P, Thijs G, Marchal K, Moreau Y, Van de Peer Y, Rouzé P, Rombauts S.

697   2002. PlantCARE, a database of plant cis-acting regulatory elements and a portal to tools for

698   in silico analysis of promoter sequences. *Nucleic Acids Research* 30:325-327 DOI:

699   10.1093/nar/30.1.325.

700   Letunic I, Bork P. 2021. Interactive Tree Of Life (iTOL) v5: an online tool for phylogenetic tree

701   display and annotation. *Nucleic Acids Research* 49:W293-W296 DOI: 10.1093/nar/gkab301.

702   Lezhneva L, Kiba T, Feria-Bourrellier AB, Lafouge F, Boutet-Mercey S, Zoufan P, Sakakibara

703   H, Daniel-Vedele F, Krapp A. 2014. The Arabidopsis nitrate transporter NRT2.5 plays a role

704   in nitrate acquisition and remobilization in nitrogen-starved plants. *Plant Journal* 80:230-241

705   DOI: 10.1111/tpj.12626.

706   Li W, Wang Y, Okamoto M, Crawford NM, Siddiqi MY, Glass AD. 2007. Dissection of the

707   AtNRT2.1:AtNRT2.2 inducible high-affinity nitrate transporter gene cluster. *Plant Physiology*

708   143:425-433 DOI: 10.1104/pp.106.091223.

709   Li Y, Li J, Yan Y, Liu W, Zhang W, Gao L, Tian Y. 2018. Knock-Down of CsNRT2.1, a

710   Cucumber Nitrate Transporter, Reduces Nitrate Uptake, Root length, and Lateral Root

711   Number at Low External Nitrate Concentration. *Frontiers in Plant Science* 9:722 DOI:

712   10.3389/fpls.2018.00722.

713   Li Z, Wang X, Cao X, Chen B, Ma C, Lv J, Sun Z, Qiao K, Zhu L, Zhang C, Fan S, Ma Q. 2021.

714   GhTULP34, a member of tubby-like proteins, interacts with GhSKP1A to negatively regulate

715   plant osmotic stress. *Genomics* 113:462-474 DOI: 10.1016/j.ygeno.2020.09.024.

716   Liu X, Huang D, Tao J, Miller AJ, Fan X, Xu G. 2014. Identification and functional assay of the

717   interaction motifs in the partner protein OsNAR2.1 of the two-component system for high-

718   affinity nitrate transport. *New Phytologist* 204:74-80 DOI: 10.1111/nph.12986.

719   Lupini A, Mercati F, Araniti F, Miller AJ, Sunseri F, Abenavoli MR. 2016. NAR2.1/NRT2.1

720   functional interaction with NO3(-) and H(+) fluxes in high-affinity nitrate transport in maize

721   root regions. *Plant Physiology and Biochemistry* 102:107-114 DOI:

722   10.1016/j.plaphy.2016.02.022.

723   Magwanga RO, Kirungu JN, Lu P, Cai X, Zhou Z, Xu Y, Hou Y, Agong SG, Wang K, Liu F.

724   2019. Map-Based Functional Analysis of the GhNLP Genes Reveals Their Roles in Enhancing

725   Tolerance to N-Deficiency in Cotton. *International Journal of Molecular Sciences* 20:4953
726   DOI: 10.3390/ijms20194953.

727 Mehari TG, Xu Y, Magwanga RO, Umer MJ, Shiraku ML, Hou Y, Wang Y, Wang K, Cai X,
728   Zhou Z, Liu F. 2021. Identification and functional characterization of Gh_D01G0514
729   (GhNAC072) transcription factor in response to drought stress tolerance in cotton. *Plant*
730   *Physiology and Biochemistry* 166:361-375 DOI: 10.1016/j.plaphy.2021.05.050.

731 Ondzighi-Assoume CA, Chakraborty S, Harris JM. 2016. Environmental Nitrate Stimulates
732   Abscisic Acid Accumulation in Arabidopsis Root Tips by Releasing It from Inactive Stores.
733   *The Plant Cell* 28:729-745 DOI: 10.1105/tpc.15.00946.

734 Orsel M, Krapp A, Daniel-Vedele F. 2002. Analysis of the NRT2 nitrate transporter family in
735   Arabidopsis. Structure and gene expression. *Plant Physiology* 129:886-896 DOI:
736   10.1104/pp.005280.

737 Ren Q, Zhou Y, Zhou X. 2020. Combined Transcriptome and Proteome Analysis of Masson Pine
738   (Pinus massoniana Lamb.) Seedling Root in Response to Nitrate and Ammonium
739   Supplementations. *International Journal of Molecular Sciences* 21:7548 DOI:
740   10.3390/ijms21207548.

741 Schmittgen TD, Livak KJ. 2008. Analyzing real-time PCR data by the comparative C(T)
742   method. *Nature Protocols* 3:1101-1108 DOI: 10.1038/nprot.2008.73.

743 Singh P, Singh RK, Song QQ, Li HB, Yang LT, Li YR. 2020. Methods for Estimation of
744   Nitrogen Components in Plants and Microorganisms. *Methods in Molecular Biology*
745   2057:103-112. DOI: 10.1007/978-1-4939-9790-9_10Tong J, Walk TC, Han P, Chen L, Shen
746   X, Li Y, Gu C, Xie L, Hu X, Liao X, Qin L. 2020. Genome-wide identification and analysis of
747   high-affinity nitrate transporter 2 (NRT2) family genes in rapeseed (Brassica napus L.) and
748   their responses to various stresses. *BMC Plant Biology* 20:464 DOI: 10.1186/s12870-020-
749   02648-1.

750 Trueman LJ, Richardson A, Forde BG. 1996. Molecular cloning of higher plant homologues of
751   the high-affinity nitrate transporters of Chlamydomonas reinhardtii and Aspergillus nidulans.
752   *Gene* 175:223-231 DOI: 10.1016/0378-1119(96)00154-0.

753 Vega A, O'Brien JA, Gutiérrez RA. 2019. Nitrate and hormonal signaling crosstalk for plant
754   growth and development. *Current Opinion in Plant Biology* 52:155-163 DOI:
755   10.1016/j.pbi.2019.10.001.

756 Wang C, Zhang W, Li Z, Li Z, Bi Y, Crawford NM, Wang Y. 2018. FIP1 Plays an Important
757   Role in Nitrate Signaling and Regulates CIPK8 and CIPK23 Expression in Arabidopsis.
758   *Frontiers in Plant Science* 9:593 DOI: 10.3389/fpls.2018.00593.

759 Wang Y, Branicky R, Noë A, Hekimi S. 2018. Superoxide dismutases: Dual roles in controlling
760   ROS damage and regulating ROS signaling. *Journal of Cell Biology* 217:1915-1928 DOI:
761   10.1083/jcb.201708007.

762 Wang Y, Tang H, Debarry JD, Tan X, Li J, Wang X, Lee TH, Jin H, Marler B, Guo H, Kissinger
763   JC, Paterson AH. 2012. MCScanX: a toolkit for detection and evolutionary analysis of gene
764   synteny and collinearity. *Nucleic Acids Research* 40:e49 DOI: 10.1093/nar/gkr1293.

765 Wei J, Zheng Y, Feng H, Qu H, Fan X, Yamaji N, Ma JF, Xu G. 2018. OsNRT2.4 encodes a
766   dual-affinity nitrate transporter and functions in nitrate-regulated root growth and nitrate
767   distribution in rice. *Journal of Experimental Botany* 69:1095-1107 DOI: 10.1093/jxb/erx486.
768 Wilkins MR, Gasteiger E, Bairoch A, Sanchez JC, Williams KL, Appel RD, Hochstrasser DF.
769   1999. Protein identification and analysis tools in the ExPASy server. *Methods in Molecular*
770   *Biology* 112:531-552 DOI: 10.1385/1-59259-584-7:531.
771 Wirth J, Chopin F, Santoni V, Viennois G, Tillard P, Krapp A, Lejay L, Daniel-Vedele F, Gojon
772   A. 2007. Regulation of root nitrate uptake at the NRT2.1 protein level in Arabidopsis thaliana.
773   *Journal of Biologica Chemistry* 282:23541-23552 DOI: 10.1074/jbc.M700901200.
774 Xiao S, Wu C, Zuo D, Cheng H, Zhang Y, Wang Q, Lv L, Song G. 2022. Systematic analysis
775   and comparison of CaLB genes reveal the functions of GhCaLB42 and GhCaLB123 in fiber
776   development and abiotic stress in cotton. *Industrial Crops and Products* 184:115030 DOI:
777   10.1016/j.indcrop.2022.115030.
778 Xie Y, Zhou Q, Zhao Y, Li Q, Liu Y, Ma M, Wang B, Shen R, Zheng Z, Wang H. 2020. FHY3
779   and FAR1 Integrate Light Signals with the miR156-SPL Module-Mediated Aging Pathway to
780   Regulate Arabidopsis Flowering. *Molecular Plant* 13:483-498 DOI:
781   10.1016/j.molp.2020.01.013.
782 Xu G, Fan X, Miller AJ. 2012. Plant nitrogen assimilation and use efficiency. *Annual Review of*
783   *Plant Biology* 63:153-182 DOI: 10.1146/annurev-arplant-042811-105532.
784 Yan M, Fan X, Feng H, Miller AJ, Shen Q, Xu G. 2011. Rice OsNAR2.1 interacts with
785   OsNRT2.1, OsNRT2.2 and OsNRT2.3a nitrate transporters to provide uptake over high and
786   low concentration ranges. *Plant Cell and Environment* 34:1360-1372 DOI: 10.1111/j.1365-
787   3040.2011.02335.x.
788 Yang W, Yu M, Zou C, Lu C, Yu D, Cheng H, Jiang P, Feng X, Zhang Y, Wang Q, Zhang H,
789   Song G, Zhou Z. 2019. Genome-wide comparative analysis of RNA-binding Glycine-rich
790   protein family genes between Gossypium arboreum and Gossypium raimondii. *PLoS One*
791   14:e218938 DOI: 10.1371/journal.pone.0218938.
792 You L, Wang Y, Zhang T, Zhu Y, Ren N, Jiang X, Zhou Y. 2022. Genome-wide identification
793   of nitrate transporter 2 (NRT2) gene family and functional analysis of MeNRT2.2 in cassava
794   (Manihot esculenta Crantz). *Gene* 809:146038 DOI: 10.1016/j.gene.2021.146038.
795 Yu J, Jung S, Cheng CH, Ficklin SP, Lee T, Zheng P, Jones D, Percy RG, Main D. 2014.
796   CottonGen: a genomics, genetics and breeding database for cotton research. *Nucleic Acids*
797   *Research* 42:D1229-D1236 DOI: 10.1093/nar/gkt1064.
798 Zhang F, He W, Yuan Q, Wei K, Ruan L, Wang L, Cheng H. 2021. Transcriptome analysis
799   identifies CsNRT genes involved in nitrogen uptake in tea plants, with a major role of
800   CsNRT2.4. *Plant Physiology and Biochemistry* 167:970-979 DOI:
801   10.1016/j.plaphy.2021.09.024.
802 Zhao L, Wang Y. 2017. Nitrate Assay for Plant Tissues. *Bio Protocol* 7:e2029 DOI:
803   10.21769/BioProtoc.2029.
804 Zhou T, Wu P, Yue C, Huang J, Zhang Z, Hua Y. 2022. Transcriptomic Dissection of
805   Allotetraploid Rapeseed (Brassica napus L.) in Responses to Nitrate and Ammonium Regimes

806   and Functional Analysis of BnaA2.Gln1;4 in Arabidopsis. *Plant and Cell Physiology* 63:755-
807   769 DOI: 10.1093/pcp/pcac037.
808

Figure 1

Phylogenetic analysis of NRT2 proteins.

The phylogenetic tree was constructed using the neighbor-joining (NJ) method in MEGA 7.0 software. Different groups were marked with different colors. AT: *A. thaliana*, Gr: *G. raimondii*, Ga: *G. arboreum*, Gh: *G. hirsutum* and Gb: *G. barbadense*.
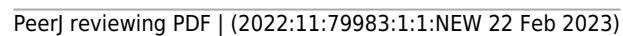
Figure 2

Chromosomal location of *GhNRT2* genes in *G. hirsutum*.

The chromosomal locations of the *GhNRT2* genes were mapped by TBtools software. The black lines indicate the location of the genes on the chromosomes. The scale bar indicates the chromosome length in the base pair (bp).
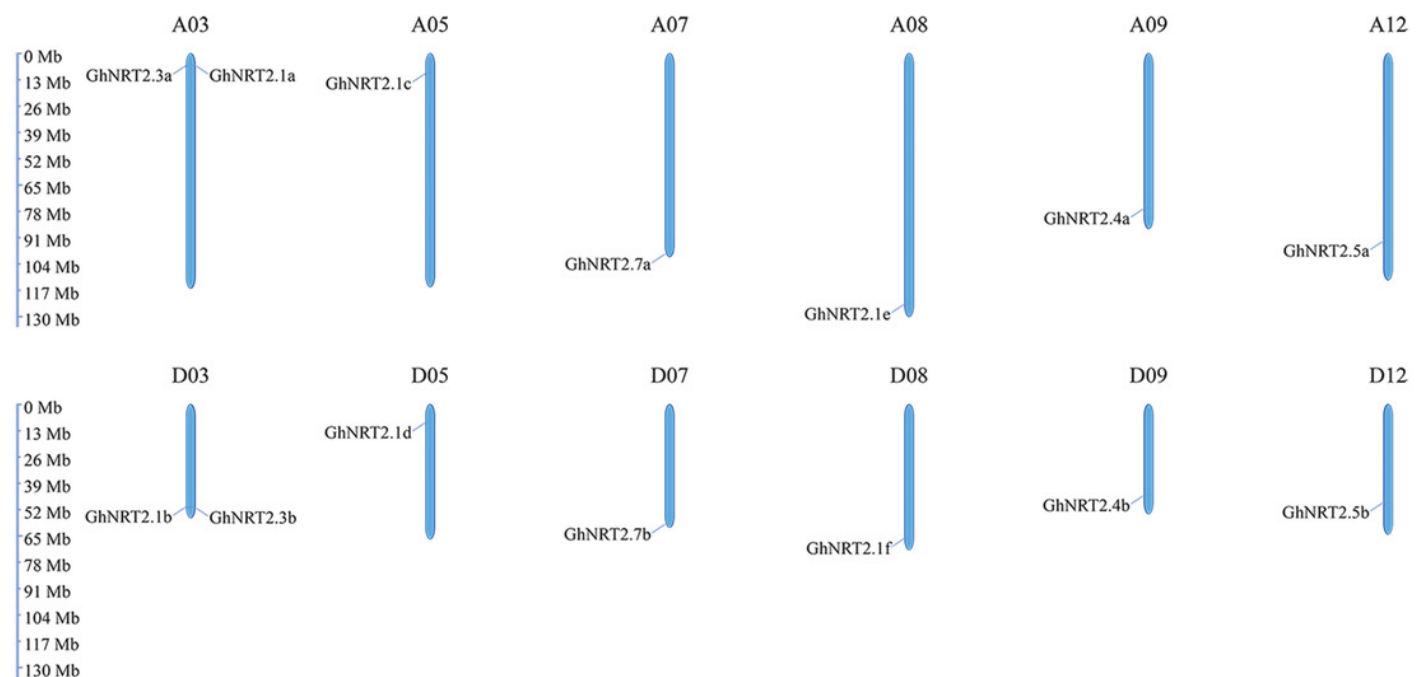
Figure 3

Syntenic relationship of *NRT2* genes in *G.harsutum*, *G.barbadense*, *G.arboreum*, and *G.raimondii*.

The syntenic relationships of the *NRT2* genes were mapped by the MCScanX program in TBtools software. The lines represented by various colors indicate the syntenic regions around the *NRT2* genes. Gr: *G. raimondii*, Ga: *G. arboreum*, Gh: *G. hirsutum* and Gb: *G. barbadense*.
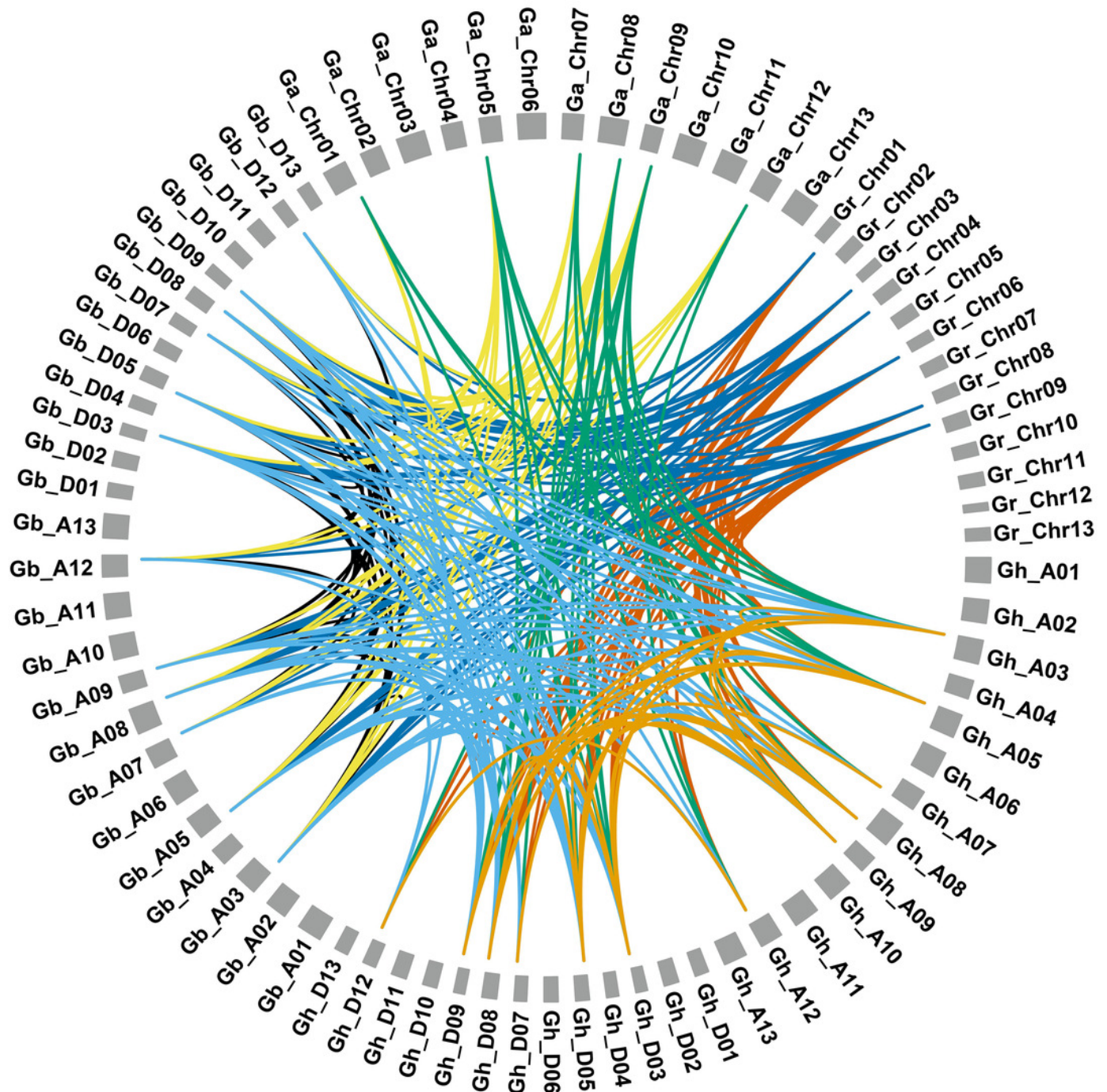
Figure 4

Phylogenetic relationship, conserved motifs, gene structure, and multiple sequence alignment of GhNRT2 proteins.

(A) Phylogenetic analysis of GhNRT2 proteins. (B) Conserved motifs of GhNRT2 proteins. The MEME software identified the conserved motifs. Different colored boxes represented different motifs. (C) Exon-intron structures of the *GhNRT2* genes. Gene structure was analyzed by GSDS software. (D) Multiple sequence alignment of GhNRT2 proteins. Amino acid sequence alignment was performed by DNAMAN software. MFS motifs and NNP motifs were boxed in red.
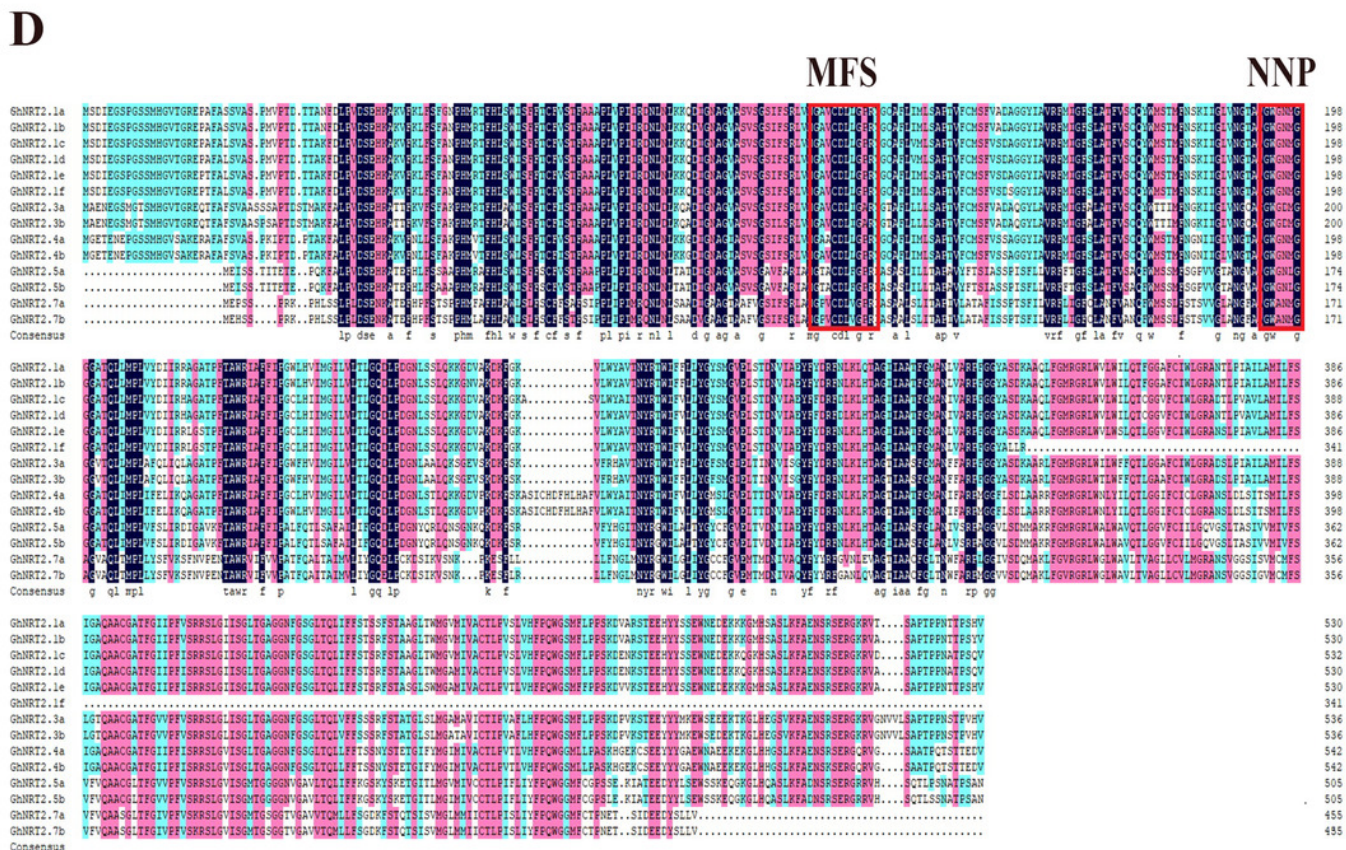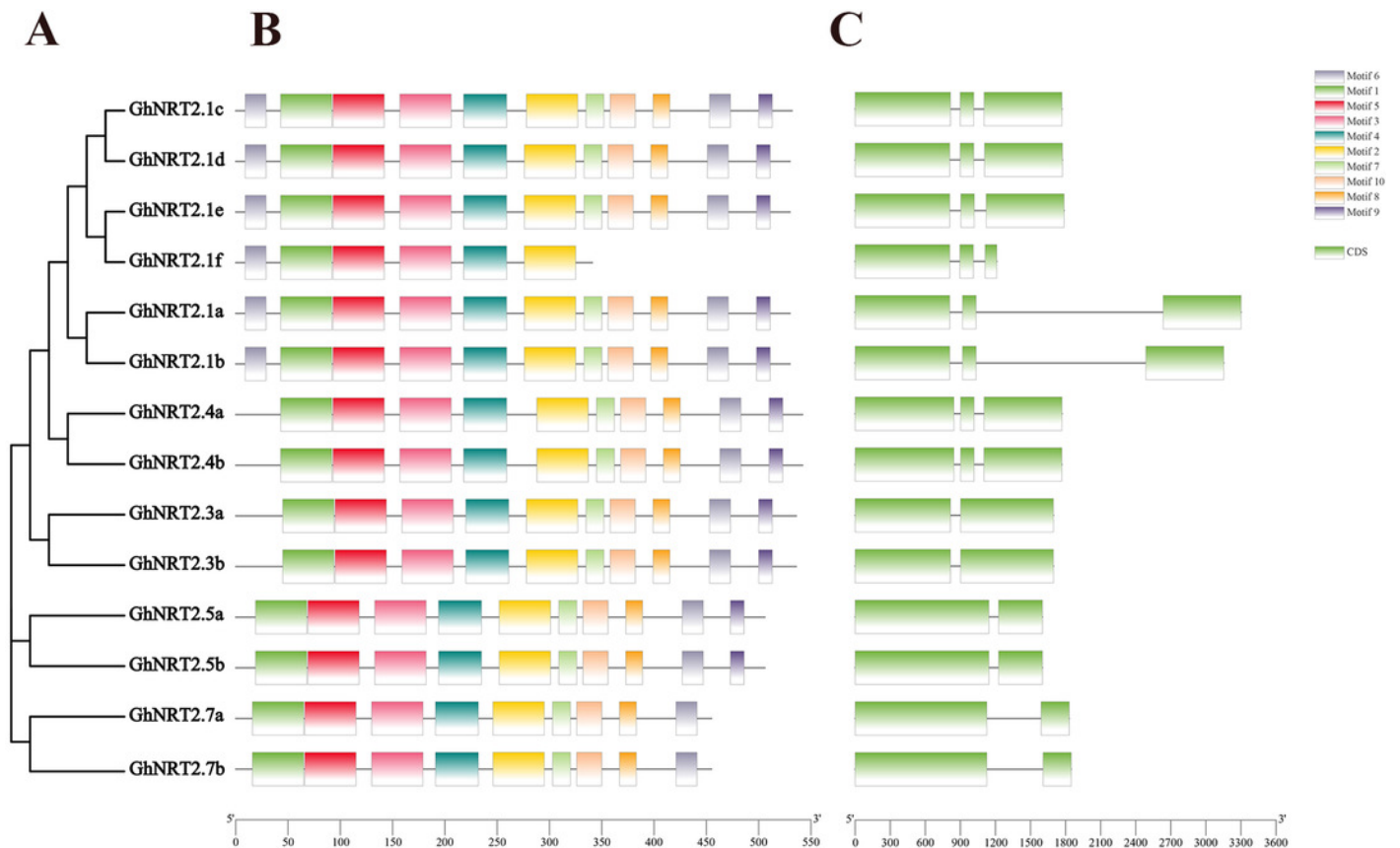
Figure 5

Predicted cis-acting elements in the promoters of *GhNRT2* genes.

The cis-acting elements were predicted from the PlantCARE database. Different colored boxes represented different cis-acting elements.
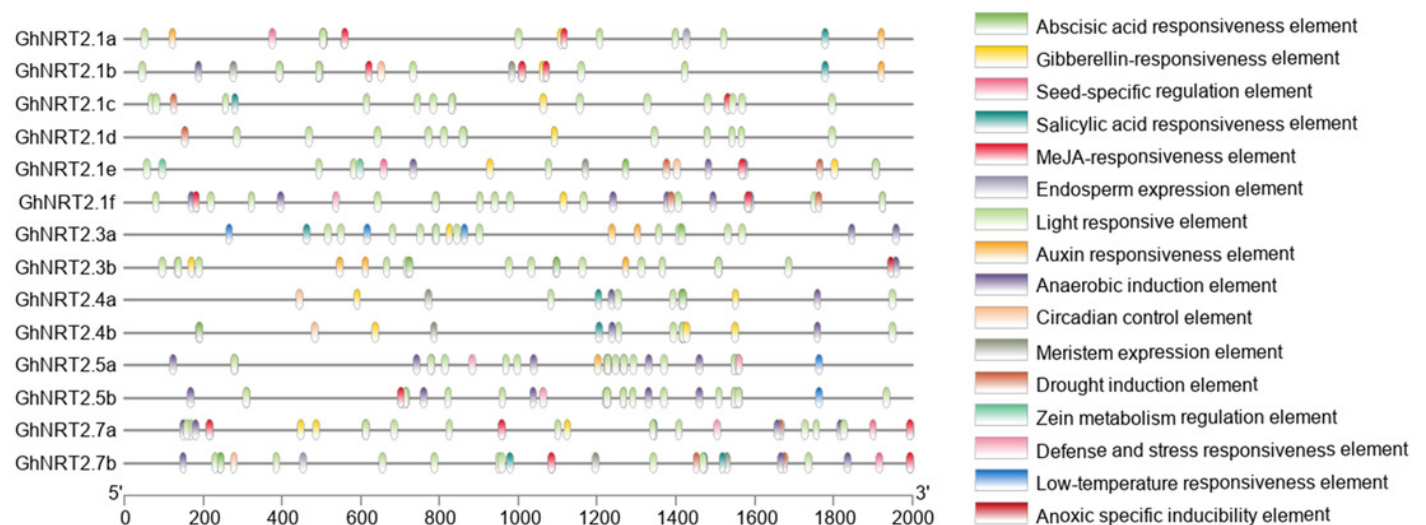
Figure 6

RNA-seq data heat map of *GhNRT2* genes expression in eleven different tissues.

The differences in expression of the *GhNRT2* genes are shown in different colors. DPA: days post anthesis.
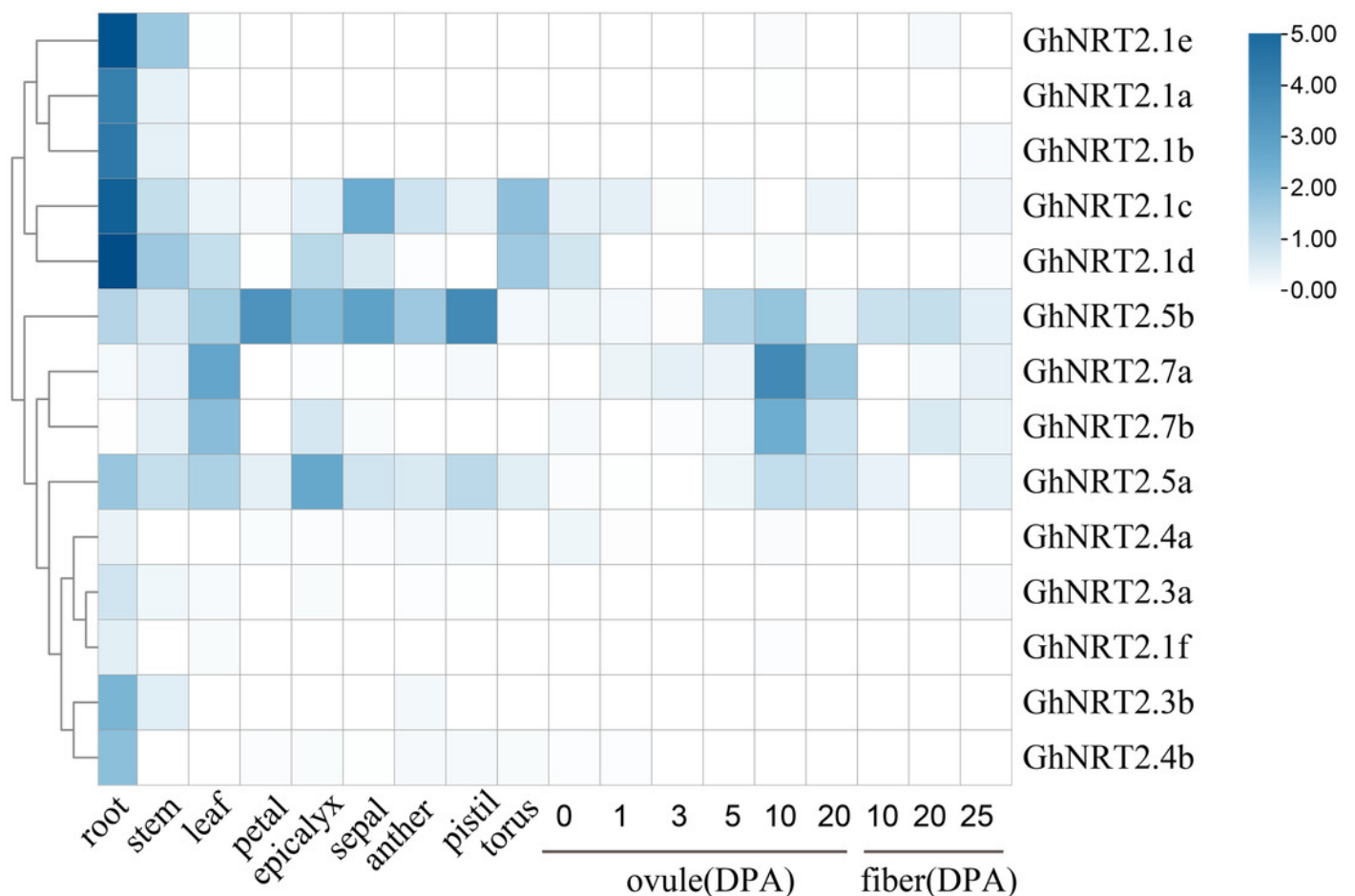
Figure 7

The relative expression levels of *GhNRT2* genes in root, stem, and leaf were determined by qRT-PCR.

GhNRT2.1a expression in roots was set to 1 and used as a control to reflect the relative expression of the *GhNRT2* genes in roots, stems, and leaves. The *GhActin* gene was used as the internal reference gene.
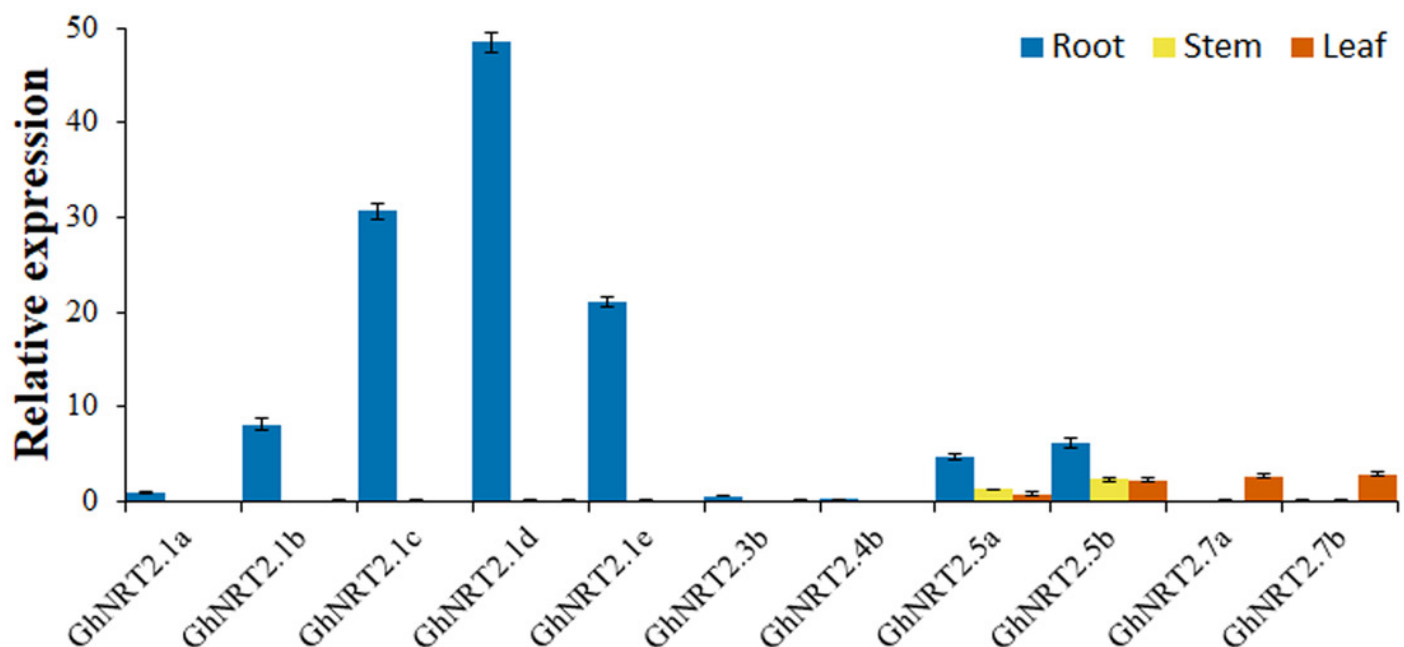
Figure 8

The relative expression levels of *GhNRT2* genes were analyzed by qRT-PCR under low nitrate conditions.

Cotton seedlings were grown in a nitrogen-free nutrient solution for one week and then resupplied with 0.25 mM NO_3^-. Root tissues were collected at 0, 1, 3, 6, 12, 24, and 48 h after treatment, respectively. The *GhActin* gene was used as the internal control.
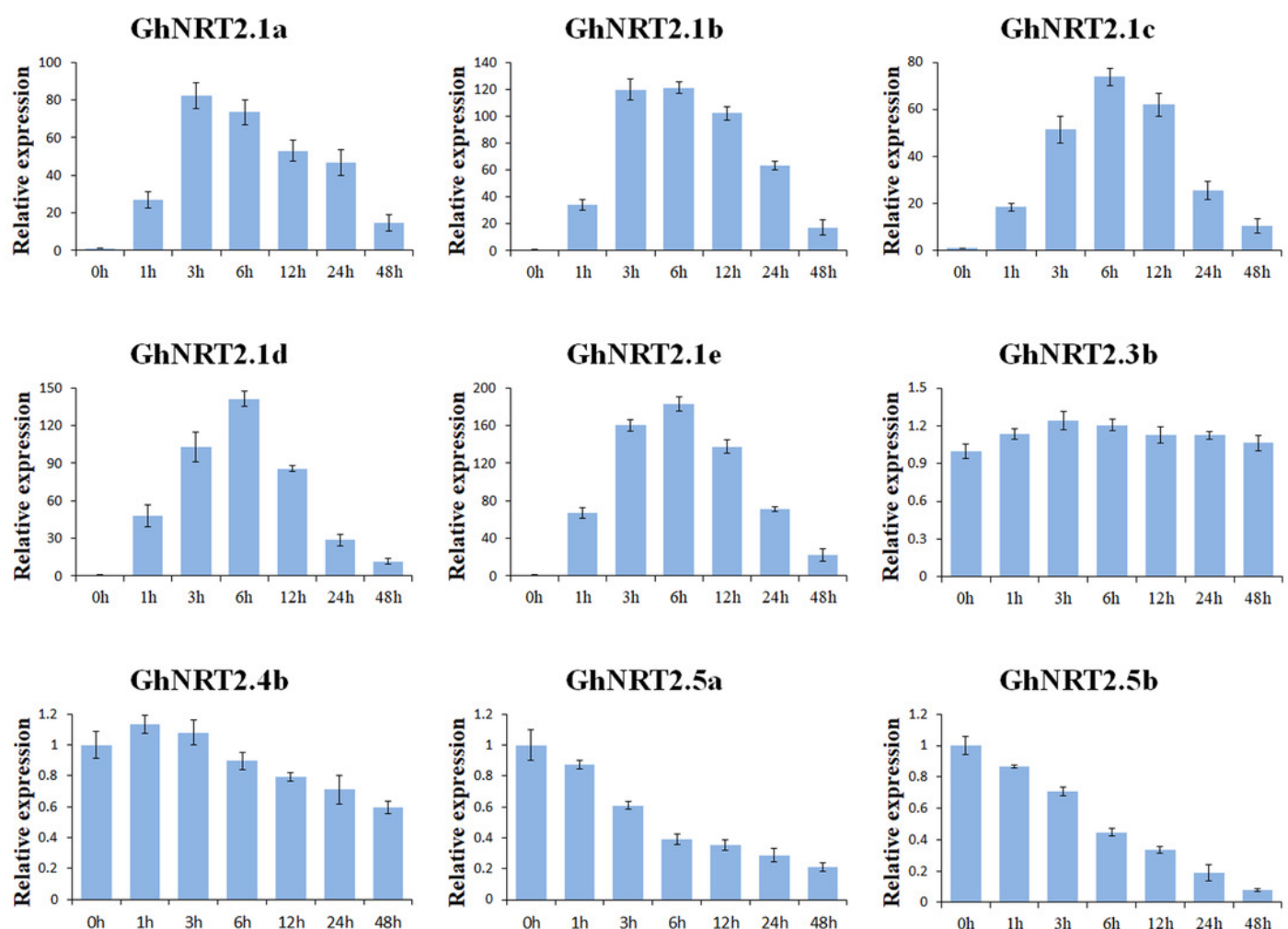
Figure 9

Phenotypic observation and identification of *GhNRT2.1e*-overexpressed *Arabidopsis*.

(A) Phenotypes of wild-type (WT) and overexpression lines grown under 0.25 mM nitrate conditions. Each small pot contained three plants. (B) The relative expression levels of *GhNRT2.1e* in wild-type (WT) and three T2 generations overexpressed lines were analyzed by qRT-PCR under normal nitrate conditions. The *AtActin* gene was used as the internal control. Quantitative determination of biomass (C), total nitrogen content (D), nitrate content (E), and total nitrogen accumulation (F) of WT and overexpression lines. The values are means ± standard deviation (SD) of ten replicates. Student's *t*-test was used to analyze the significance of differences. *$P < 0.05$ and **$P < 0.01$ indicate significant differences between WT and overexpression lines. "CK" represents a nutrient solution with a nitrate concentration of 2.5 mM; "Low Nitrate" represents a nutrient solution with a nitrate concentration of 0.25 mM; "WT" represents the wild type; "OE" represents overexpression line.
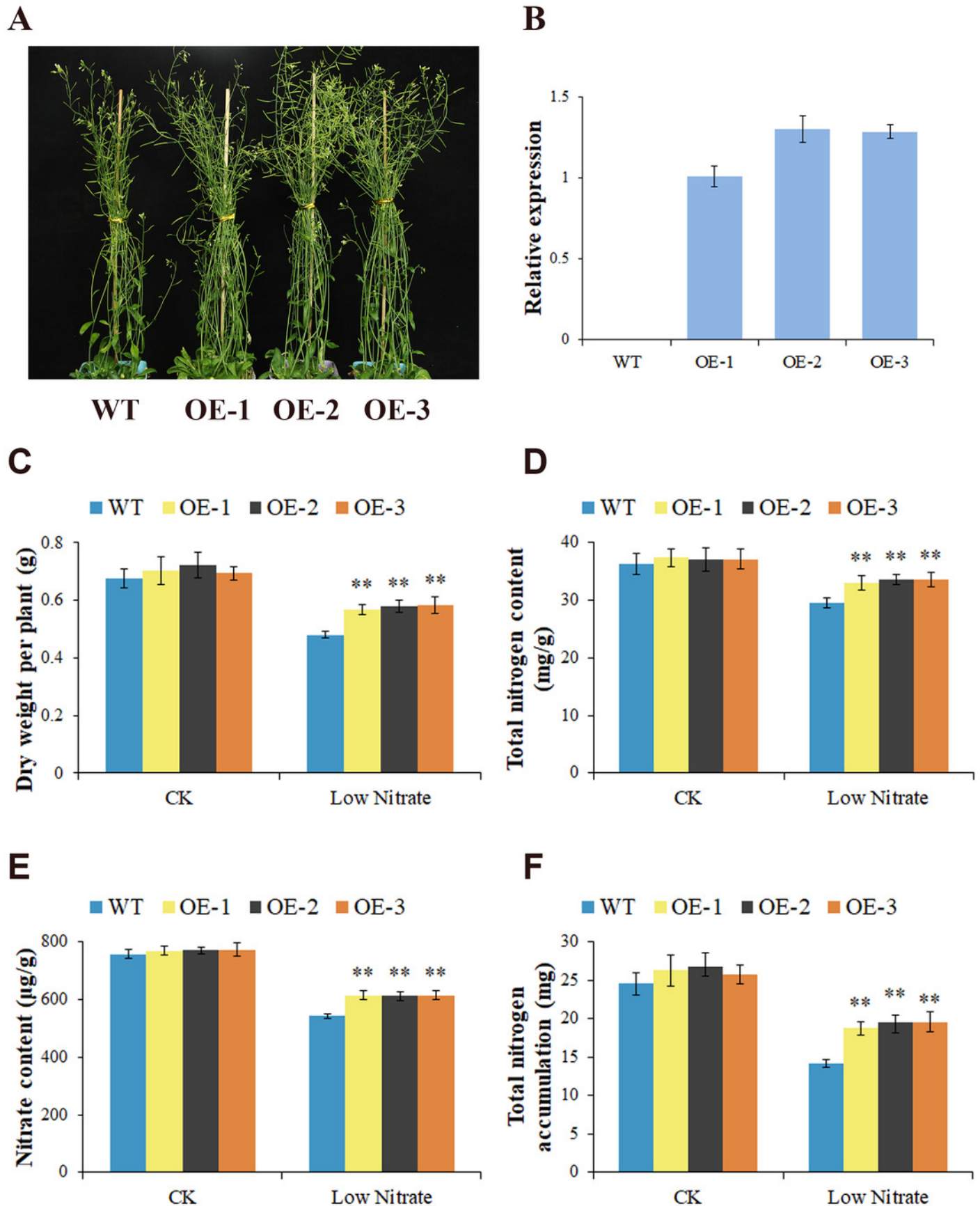
Figure 10

Physiological and biochemical analysis of *GhNRT2.1e*-overexpressed *Arabidopsis*.

Nitrogen uptake efficiency (NUpE) (A), nitrogen utilization efficiency (NUtE) (B), Nitrate reductase (NR) activity (C), Glutamine synthetase (GS) activity (D), Glutamate synthetase (GOGAT) activity (E), and amino acid content (F) of WT and overexpression lines grown under 2.5 mM NO_3^- and 0.25 mM NO_3^- conditions. The values are means ± standard deviation (SD) of ten replicates. Student's *t*-test was used to analyze the significance of differences. *$P <$ 0.05 and **$P <$ 0.01 indicate significant differences between WT and overexpression lines. "CK" represents a nutrient solution with a nitrate concentration of 2.5 mM; "Low Nitrate" represents a nutrient solution with a nitrate concentration of 0.25 mM; "WT" represents the wild type; "OE" represents overexpression line.
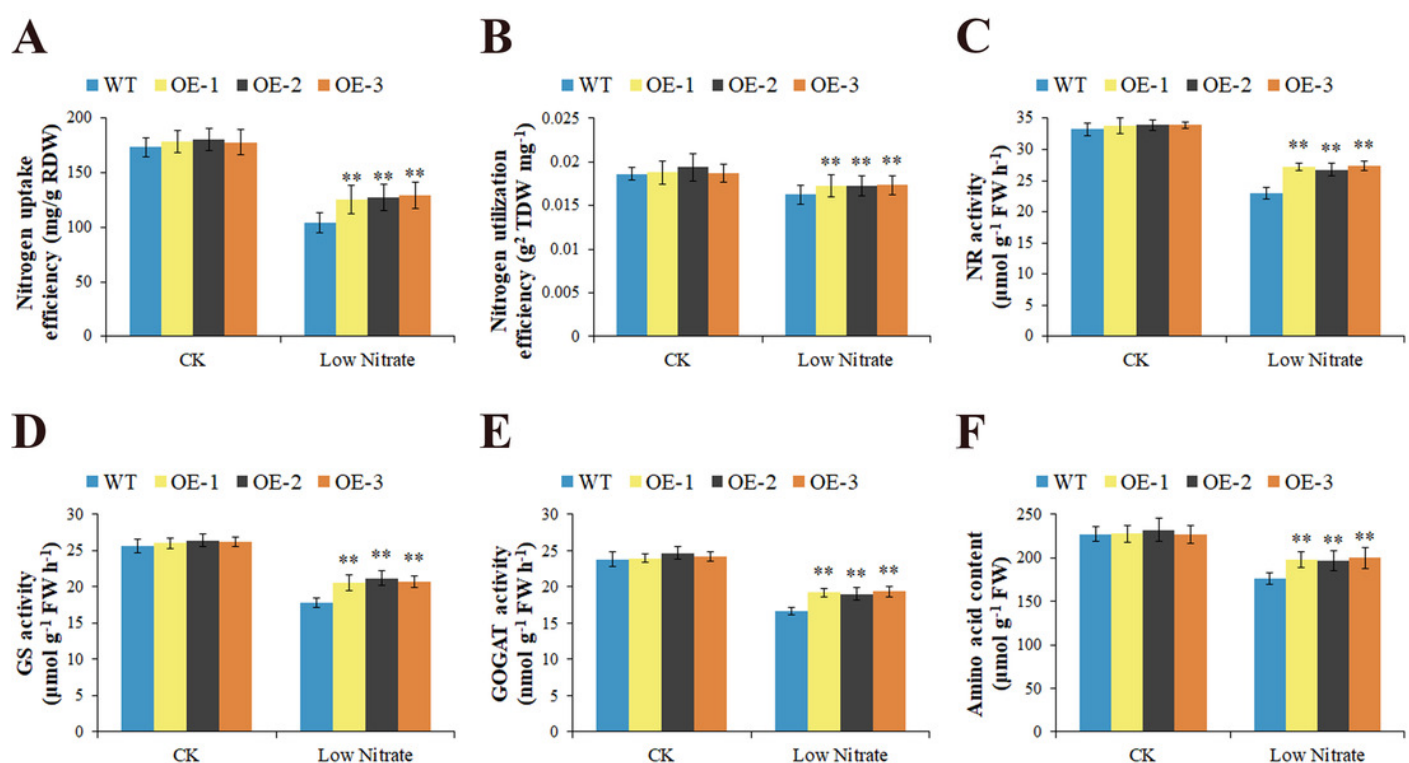
Figure 11

Phenotypic observation and identification of silenced plants.

(A) Albino phenotype appearance on the leaves of the TRV2:PDS infused plants. (B) The phenotype of WT, TRV2:00, and TRV2:GhNRT2.1e plants grown at 0.25 mM nitrate concentration. (C) The expression levels of *GhNRT2.1e* in WT, TRV2:00, and TRV2:GhNRT2.1e plants grown at 0.25 mM and 2.5 mM nitrate concentrations were analyzed by qRT-PCR. The *GhActin* gene was used as the internal control. Comparison of dry weight (D), total nitrogen content (E), and nitrate content (F) of WT, TRV2:00, and TRV2:GhNRT2.1e plants. The values are means ± standard deviation (SD) of ten replicates. Student's *t*-test was used to analyze the significance of differences. *$P < 0.05$ and **$P < 0.01$ indicate significant differences between *GhNRT2.1e*-silenced plants and control plants. "WT" represents the wild type; "TRV2:00" represents the plants carrying control the TRV2 empty vector; "TRV2:GhNRT2.1e" represents the *GhNRT2.1e*-silenced plants; "CK" represents a nutrient solution with a nitrate concentration of 2.5 mM; "Low Nitrate" represents a nutrient solution with a nitrate concentration of 0.25 mM.
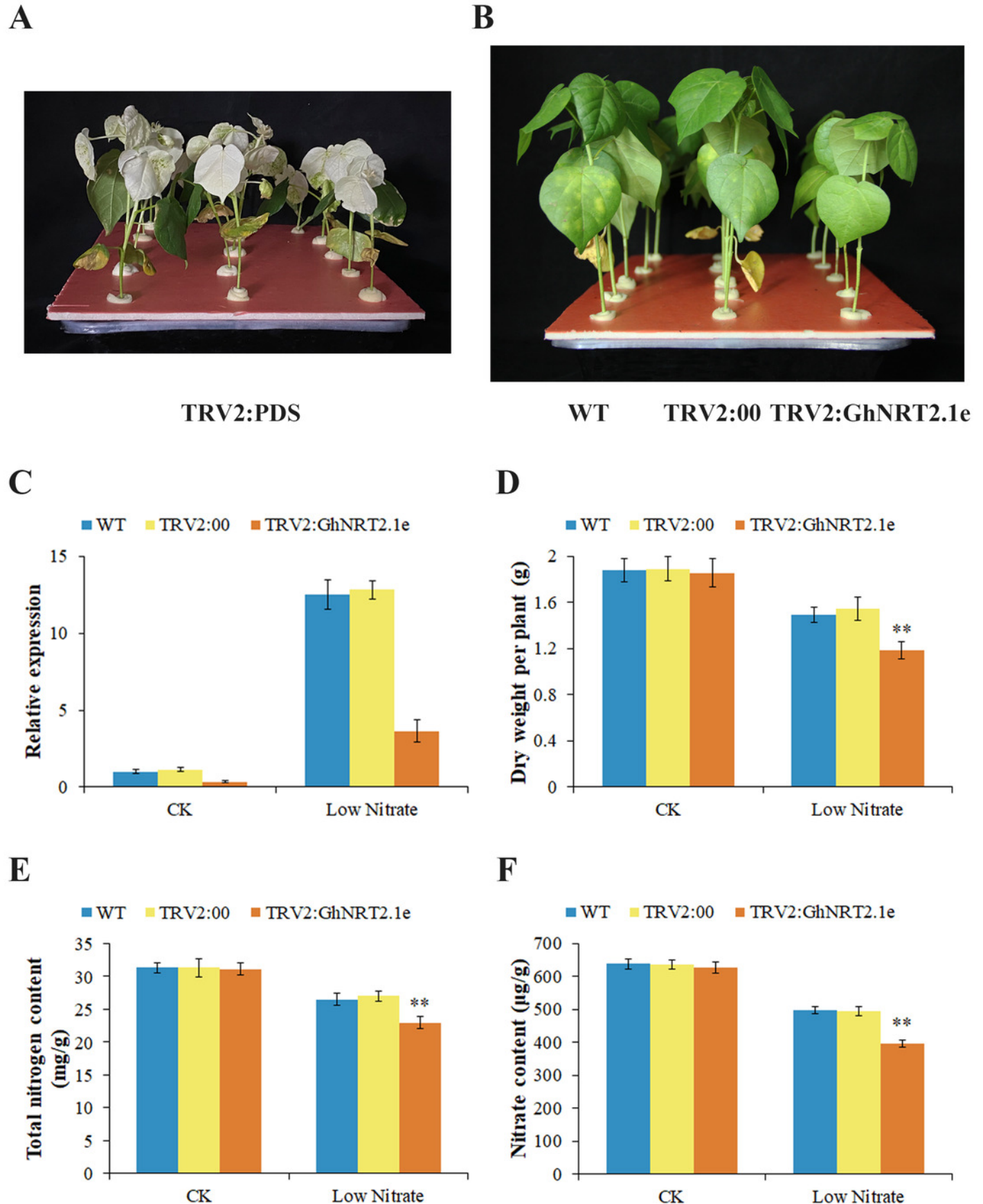
Figure 12

Physiological and biochemical evaluation of *GhNRT2.1e*-VIGS cotton plants.

Quantitative determination of nitrogen uptake efficiency (NUpE) (A), nitrogen utilization efficiency (NUtE) (B), total nitrogen accumulation (C), chlorophyll content (D), Nitrate reductase (NR) activity (E), Glutamine synthetase (GS) activity (F), Glutamate synthetase (GOGAT) activity (G), amino acid content (H), catalase (CAT) activity (I), peroxidase (POD) activity (J), superoxide dismutase (SOD) activity (K) and malondialdehyde (MDA) concentration (L) in *GhNRT2.1e*-silenced and control plants grown under 2.5 mM NO_3^- and 0.25 mM NO_3^- conditions. The values are means ± standard deviation (SD) of ten replicates. Student's *t*-test was used to analyze the significance of differences. *$P < 0.05$ and **$P < 0.01$ indicate significant differences between *GhNRT2.1e*-silenced plants and control plants. "WT" represents the wild type; "TRV2:00" represents the plants carrying control the TRV2 empty vector; "TRV2:GhNRT2.1e" represents the *GhNRT2.1e*-silenced plants; "CK" represents a nutrient solution with a nitrate concentration of 2.5 mM; "Low Nitrate" represents a nutrient solution with a nitrate concentration of 0.25 mM.

A
B
C
D
E
F
G
H
I
J
K
L
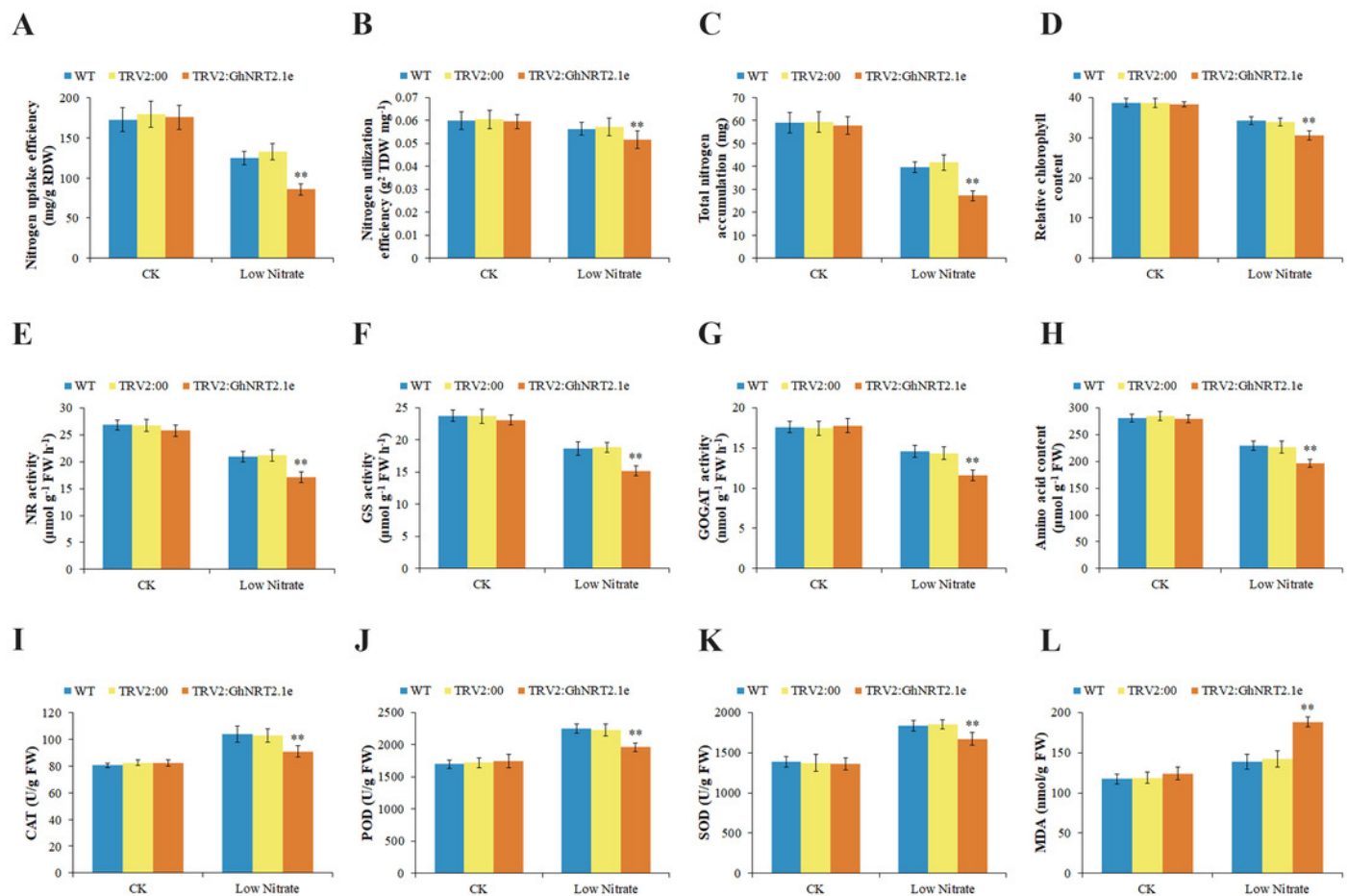
Figure 13

The interaction between GhNRT2.1e and GhNAR2.1 was verified by yeast two-hybrid assay and luciferase complementation imaging assays.

(A) Yeast cells were grown on SD-LW (SD-Leu-Trp) medium. (B) Yeast cells were grown on SD-AHLW (SD-Ade-His-Leu-Trp) medium. (C) Imaging of luciferase complementation between SPL3-nLUC and FHY3-cLUC as a positive control. (D) Imaging of luciferase complementation between GhNRT2.1e and GhNAR2.1.